PHYSICAL REVIEW D **95,** 012003 (2017)

Inclusive search for supersymmetry using razor variables in *pp* collisions at $\sqrt{s} = 13$ TeV

V. Khachatryan *et al.*[*]
(CMS Collaboration)

(Received 24 September 2016; published 6 January 2017)

An inclusive search for supersymmetry using razor variables is performed in events with four or more jets and no more than one lepton. The results are based on a sample of proton-proton collisions corresponding to an integrated luminosity of 2.3 fb^{-1} collected with the CMS experiment at a center-of-mass energy of $\sqrt{s} = 13$ TeV. No significant excess over the background prediction is observed in data, and 95% confidence level exclusion limits are placed on the masses of new heavy particles in a variety of simplified models. Assuming that pair-produced gluinos decay only via three-body processes involving third-generation quarks plus a neutralino, and that the neutralino is the lightest supersymmetric particle with a mass of 200 GeV, gluino masses below 1.6 TeV are excluded for any branching fractions for the individual gluino decay modes. For some specific decay mode scenarios, gluino masses up to 1.65 TeV are excluded. For decays to first- and second-generation quarks and a neutralino with a mass of 200 GeV, gluinos with masses up to 1.4 TeV are excluded. Pair production of top squarks decaying to a top quark and a neutralino with a mass of 100 GeV is excluded for top squark masses up to 750 GeV.

DOI: 10.1103/PhysRevD.95.012003

I. INTRODUCTION

Supersymmetry (SUSY) is a proposed extended space-time symmetry that introduces a bosonic (fermionic) partner for every fermion (boson) in the standard model (SM) [1–9]. Supersymmetric extensions of the SM are particularly compelling because they yield solutions to the gauge hierarchy problem without the need for large fine-tuning of fundamental parameters [10–15], exhibit gauge coupling unification [16–21], and can provide weakly interacting particle candidates for dark matter [22,23]. For SUSY to provide a "natural" solution to the gauge hierarchy problem, the three Higgsinos, two neutral and one charged, must be light, and two top squarks, one bottom squark, and the gluino must have masses below a few TeV, making them potentially accessible at the CERN LHC. Previous searches for SUSY by the CMS [24–30] and ATLAS [31–37] collaborations have probed SUSY particle masses near the TeV scale, and the increase in the center-of-mass energy of the LHC from 8 to 13 TeV provides an opportunity to significantly extend the sensitivity to higher SUSY particle masses [38–51].

In R-parity [52] conserving SUSY scenarios, the lightest SUSY particle (LSP) is stable and assumed to be weakly interacting. For many of these models, the experimental signatures at the LHC are characterized by an abundance of jets and a large transverse momentum imbalance, but the exact form of the final state can vary significantly, depending on the values of the unconstrained model parameters. To ensure sensitivity to a broad range of SUSY parameter space, we adopt an inclusive search strategy, categorizing events according to the number of identified leptons and b-tagged jets. The razor kinematic variables M_{R} and R^2 [53,54] are used as search variables and are generically sensitive to pair production of massive particles with subsequent direct or cascading decays to weakly interacting stable particles. Searches for SUSY and other beyond the SM phenomena using razor variables have been performed by both the CMS [53–58] and ATLAS [59,60] collaborations in the past.

We interpret the results of the inclusive search using simplified SUSY scenarios for pair production of gluinos and top squarks. First, we consider models in which the gluino undergoes three-body decay, either to a bottom or top quark-antiquark pair and the lightest neutralino $\tilde{\chi}_1^0$, assumed to be the lightest SUSY particle, or to a bottom quark (antiquark), a top antiquark (quark), and the lightest chargino $\tilde{\chi}_1^{\pm}$, assumed to be the next-to-lightest SUSY particle (NLSP). The NLSP is assumed to have a mass that is 5 GeV larger than the mass of the LSP, motivated by the fact that in many natural SUSY scenarios the lightest chargino and the two lightest neutralinos are Higgsino-like and quasidegenerate [61]. The NLSP decays to an LSP and an off-shell W boson, the decay products of which mostly have too low momentum to be identifiable. The specific choice of the NLSP-LSP mass splitting does not have a large impact on the results of the interpretation. The full range of branching fractions to the three possible decay

[*]Full author list given at the end of the article.

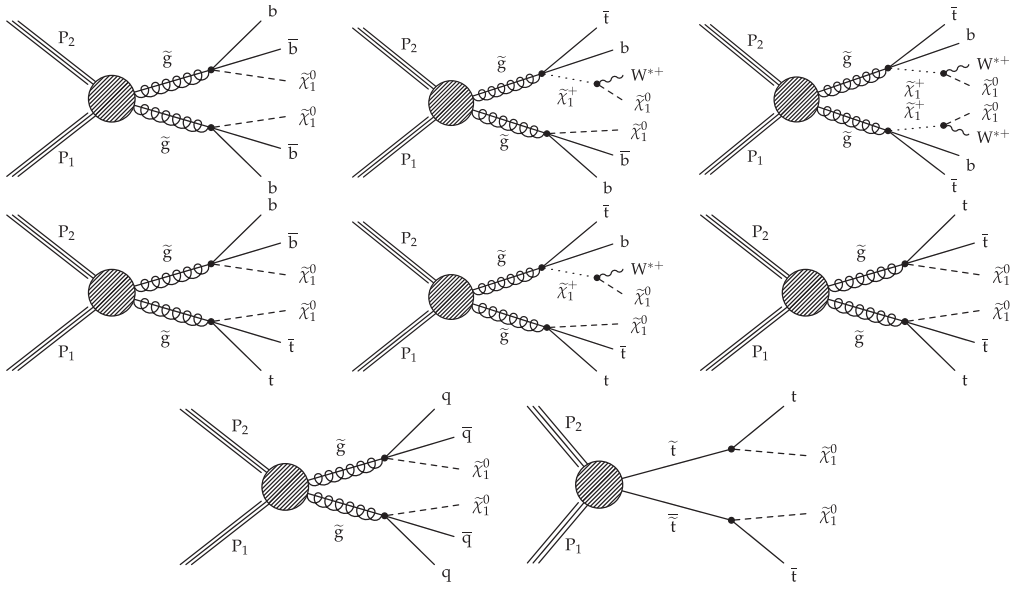

FIG. 1. Diagrams displaying the distinct event topologies of gluino (all but last) and top squark (last) pair production considered in this paper. Diagrams corresponding to charge conjugate decay modes are implied. The symbol W^* is used to denote a virtual W boson.

modes ($b\bar{b}\tilde{\chi}_1^0$, $b\bar{t}\tilde{\chi}_1^+$ or $\bar{b}t\tilde{\chi}_1^-$, and $t\bar{t}\tilde{\chi}_1^0$) is considered, assuming that these sum to 100%. We also consider a model in which the gluino decays to a first- or second-generation quark-antiquark pair and the LSP. Finally, we consider top squark pair production with the top squark decaying to a top quark and the LSP. Diagrams of these simplified model processes are shown in Fig. 1.

This paper is organized as follows. Section II presents an overview of the CMS detector. A description of simulated signal and background samples is given in Sec. III. Section IV describes physics object reconstruction and the event selection. Section V describes the analysis strategy and razor variables, and the background estimation techniques used in this analysis are described in Sec. VI. Section VII covers the systematic uncertainties. Finally, our results and their interpretation are presented in Sec. VIII, followed by a summary in Sec. IX.

II. CMS DETECTOR

The central feature of the CMS detector is a superconducting solenoid of 6 m internal diameter, providing a magnetic field of 3.8 T. Within the solenoid volume are a silicon pixel and a silicon strip tracker, a lead tungstate crystal electromagnetic calorimeter (ECAL), and a brass and scintillator hadron calorimeter (HCAL), each comprising a barrel and two end cap sections. Muons are measured in gas-ionization detectors embedded in the magnet steel flux-return yoke outside the solenoid. Extensive forward calorimetry complements the coverage provided by the barrel and end cap detectors. Jets are reconstructed within the pseudorapidity region $|\eta| < 5$ covered by the ECAL and HCAL, where $\eta \equiv -\ln[\tan(\theta/2)]$ and θ is the polar angle of the trajectory of the particle with respect to the counterclockwise beam direction. Electrons and muons are reconstructed in the region with $|\eta| < 2.5$ and 2.4, respectively. Events are selected by a two-level trigger system. The first level is based on a hardware trigger, followed by a software-based high level trigger. A more detailed description of the CMS detector, together with a definition of the coordinate system used and the relevant kinematic variables, can be found in Ref. [62].

III. SIMULATED EVENT SAMPLES

Simulated Monte Carlo (MC) samples are used for modeling of the SM backgrounds in the search regions and for calculating the selection efficiencies for SUSY signal models. The production of $t\bar{t}+$ jets, $W+$ jets, $Z+$ jets, $\gamma+$ jets, and QCD multijet events, as well as the production of gluino and top squark pairs, is simulated with the MC generator MADGRAPH v5 [63]. Single top quark events are modeled at next-to-leading order (NLO) with MADGRAPH_aMC@NLO v2.2 [64] for the s-channel and with POWHEG v2 [65,66] for the t-channel and W-associated production. Contributions from $t\bar{t}W$ and $t\bar{t}Z$ are also simulated with MADGRAPH_aMC@NLO v2.2. Simulated events are interfaced with PYTHIA v8.2 [67] for fragmentation and parton showering. The NNPDF3.0LO and NNPDF3.0LO [68] parton distribution functions are used, respectively, with MADGRAPH and with POWHEG and MADGRAPH_aMC@NLO.

The SM background events are simulated using a GEANT4-based model [69] of the CMS detector. The simulation of SUSY signal model events is performed using the CMS fast simulation package [70]. All simulated events include the effects of pileup, i.e. multiple pp collisions within the same or neighboring bunch crossings,

and are processed with the same chain of reconstruction programs as is used for collision data. Simulated events are weighted to reproduce the observed distribution of pileup vertices in the data set, calculated based on the measured instantaneous luminosity.

The SUSY signal production cross sections are calculated to NLO plus next-to-leading-logarithm (NLL) accuracy [71–76], assuming all SUSY particles other than those in the relevant diagram to be too heavy to participate in the interaction. The NLO + NLL cross sections and their associated uncertainties [76] are used to derive the exclusion limits on the masses of the SUSY particles. The hard scattering is generated using MADGRAPH with up to two extra partons to model initial-state radiation at the matrix element level, and simulated events are interfaced to PYTHIA v8.2 for the showering, fragmentation, and hadronization steps.

IV. OBJECT RECONSTRUCTION AND SELECTION

Physics objects are defined using the particle-flow (PF) algorithm [77,78]. The PF algorithm reconstructs and identifies each individual particle with an optimized combination of information from the various elements of the CMS detector. All reconstructed PF candidates are clustered into jets using the anti-k_{T} algorithm [79,80] with a distance parameter of 0.4. The jet momentum is determined as the vector sum of all particle momenta in the jet, and jet-energy corrections are derived from simulation and confirmed by *in situ* measurements of the energy balance in dijet and photon + jet events. Jets are required to pass loose identification criteria on the jet composition designed to reject spurious signals arising from noise and failures in the event reconstruction [81,82]. For this search, we consider jets with transverse momentum $p_{\mathrm{T}} > 40$ GeV and $|\eta| < 3.0$. The missing transverse momentum vector $\vec{p}_{\mathrm{T}}^{\,\mathrm{miss}}$ is defined as the projection on the plane perpendicular to the beams of the negative vector sum of the momenta of all reconstructed PF candidates in an event. Its magnitude is referred to as the missing transverse energy $E_{\mathrm{T}}^{\mathrm{miss}}$.

Electrons are reconstructed by associating a cluster of energy deposited in the ECAL with a reconstructed track [83] and are required to have $p_{\mathrm{T}} > 5$ GeV and $|\eta| < 2.5$. A "tight" selection used to identify prompt electrons with $p_{\mathrm{T}} > 25$ GeV is based on requirements on the electromagnetic shower shape, the geometric matching of the track to the calorimeter cluster, the track quality and impact parameter, and isolation. The isolation of electrons and muons is defined as the scalar sum of the transverse momenta of all neutral and charged PF candidates within a cone $\Delta R = \sqrt{(\Delta\eta)^2 + (\Delta\phi)^2}$ along the lepton direction. The variable is corrected for the effects of pileup using an effective area correction [84], and the cone size ΔR shrinks with increasing lepton p_{T} according to

$$\Delta R = \begin{cases} 0.2, & p_{\mathrm{T}} \leq 50\ \mathrm{GeV} \\ 10\ \mathrm{GeV}/p_{\mathrm{T}}, & 50 < p_{\mathrm{T}} \leq 200\ \mathrm{GeV} \\ 0.05, & p_{\mathrm{T}} > 200\ \mathrm{GeV}. \end{cases} \quad (1)$$

The use of the lepton p_{T}-dependent isolation cone enhances the efficiency for identifying leptons in events containing a large amount of hadronic energy, such as those with $t\bar{t}$ production. For tight electrons, the isolation is required to be less than 10% of the electron p_{T}. The selection efficiency for tight electrons increases from 60% for p_{T} around 20 GeV to 70% for p_{T} around 40 GeV and to 80% for p_{T} above 50 GeV.

To improve the purity of all-hadronic signals in the zero-lepton event categories, a looser "veto" selection is also defined. For this selection, electrons are required to have $p_t > 5$ GeV. The output of a boosted decision tree is used to identify electrons based on shower shape and track information [83]. For electrons with $p_t > 20$ GeV, the isolation is required to be less than 20% of the electron p_{T}. For electrons with p_{T} between 5 and 20 GeV, the value of the isolation, computed by summing the p_{T}'s of all particle flow candidates within a ΔR cone of 0.3, is required to be less than 5 GeV. For the veto electron selection, the efficiency increases from 60% for p_{T} around 5 GeV to 80% for p_{T} around 15 GeV and 90% for p_{T} above 20 GeV.

Muons are reconstructed by combining tracks found in the muon system with corresponding tracks in the silicon detectors [85] and are required to have $p_t > 5$ GeV and $|\eta| < 2.4$. Muons are identified based on the quality of the track fit, the number of detector hits used in the tracking algorithm, and the compatibility between track segments. The absolute value of the 3D impact parameter significance of the muon track, which is defined as the ratio of the impact parameter to its estimated uncertainty, is required to be less than 4. As for electrons, we define a tight selection for muons with $p_t > 20$ GeV and a veto selection for muons with $p_t > 5$ GeV. For both tight and veto muons with $p_t > 20$ GeV, the isolation is required to be less than 20% of the muon p_{T}, while for veto muons with p_{T} between 5 and 20 GeV, the isolation computed using a ΔR cone of 0.4 is required to be less than 10 GeV. For tight muons, we require $d_0 < 0.2$ cm, where d_0 is the transverse impact parameter of the muon track, while this selection is not applied for veto muons. The selection efficiency for tight muons increases from 65% for p_{T} around 20 GeV to 75% for p_{T} around 40 GeV and to 80% for p_{T} above 50 GeV. For the veto muon selection, the efficiency increases from 85% for p_{T} around 5 GeV to 95% for p_{T} above 20 GeV.

We additionally reconstruct and identify hadronically decaying τ leptons (τ_{h}) to further enhance the all-hadronic purity of the zero-lepton event categories, using the hadron-plus-strips algorithm [86], which identifies τ decay modes with one charged hadron and up to two neutral pions, or three charged hadrons. The τ_{h} candidate is required to have $p_t > 20$ GeV, and the isolation, defined as the p_{T} sum of

other nearby PF candidates, must be below a certain threshold. The loose cutoff-based selection [86] is used and results in an efficiency of about 50% for successfully reconstructed τ_h decays.

To identify jets originating from b-hadron decays, we use the combined secondary vertex b jet tagger, which uses the inclusive vertex finder to select b jets [87,88]. The "medium" working point is used to define the event categories for the search signal regions. For jets with p_T between 40 and 200 GeV, the b jet tagging efficiency is approximately 70%, and the probability of misidentifying a light-flavor quark or gluon as a b jet is 1.5% in typical background events relevant for this search.

Photon candidates are reconstructed from clusters of energy deposits in the ECAL. They are identified using selections on the transverse shower width $\sigma_{\eta\eta}$ as defined in Ref. [89] and the hadronic to electromagnetic energy ratio (H/E). Photon isolation, defined as the scalar p_T sum of charged particles within a cone of $\Delta R < 0.3$, must be less than 2.5 GeV. Finally, photon candidates that share the same energy cluster as an identified electron are vetoed.

V. ANALYSIS STRATEGY AND EVENT SELECTION

We select events with four or more jets, using search categories defined by the number of leptons and b-tagged jets in the event. The Multijet category consists of events with no electrons or muons passing the tight or veto selection and no selected τ_h. Events in the one electron (muon) category, denoted as the Electron Multijet (Muon Multijet) category, are required to have one and only one electron (muon) passing the tight selection. Within these three event classes, we divide the events further into categories depending on whether the events have zero, one, two, or more than two b-tagged jets.

Each event in the above categories is treated as a dijetlike event by grouping selected leptons and jets in the event into two "megajets," the 4-momenta of which are defined as the vector sum of the 4-momenta of their constituent physics objects [55]. The clustering algorithm selects the grouping that minimizes the sum of the squares of the invariant masses of the two megajets. We define the razor variables M_R and M_T^R as

$$M_R \equiv \sqrt{(|\vec{p}^{\,j_1}| + |\vec{p}^{\,j_2}|)^2 - (p_z^{j_1} + p_z^{j_2})^2}, \quad (2)$$

$$M_T^R \equiv \sqrt{\frac{E_t^{\rm miss}(p_T^{j_1} + p_T^{j_2}) - \vec{p}_T^{\,\rm miss} \cdot (\vec{p}_T^{\,j_1} + \vec{p}_T^{\,j_2})}{2}}, \quad (3)$$

where $\vec{p}_{j_i}$, $\vec{p}_T^{\,j_i}$, and $p_z^{j_i}$ are the momentum of the ith megajet and its transverse and longitudinal components with respect to the beam axis, respectively. The dimensionless variable R is defined as

$$R \equiv \frac{M_T^R}{M_R}. \quad (4)$$

For a typical SUSY decay of a superpartner $\tilde{q}$ decaying into an invisible neutralino $\tilde{\chi}_1^0$ and the standard model partner q, the mass variable M_R peaks at a characteristic mass scale [53,54] $(m_{\tilde{q}}^2 - m_{\tilde{\chi}_1^0}^2)/m_{\tilde{\chi}_1^0}$. For standard model background processes, the distribution of M_R has an exponentially falling shape. The variable R^2 is related to the missing transverse energy and is used to suppress QCD multijet background.

The events of interest are triggered either by the presence of a high-p_T electron or muon or through dedicated hadronic triggers requiring the presence of at least two highly energetic jets and with loose thresholds on the razor variables M_R and R^2. The single-electron (single-muon) triggers require at least one isolated electron (muon) with $p_T > 23$ (20) GeV. The isolation requirement is dropped for electrons (muons) with $p_T > 105$ (50) GeV. The efficiencies for the single electron (muon) triggers are above 70% for p_T around 25 (20) GeV and reach a plateau above 97% for $p_T > 40$ GeV. The efficiencies for the single electron trigger were measured in data and simulation and found to be in good agreement, as were the corresponding efficiencies for muons. The hadronic razor trigger requires at least two jets with $p_T > 80$ GeV or at least four jets with $p_T > 40$ GeV. The events are also required to pass selections on the razor variables $M_R > 200$ GeV and $R^2 > 0.09$ and on the product $(M_R + 300\ \text{GeV}) \times (R^2 + 0.25) > 240$ GeV. The efficiency of the hadronic razor trigger for events passing the baseline M_R and R^2 selections described below is 97% and is consistent with the prediction from MC simulation.

For events in the Electron or Muon Multijet categories, the search region is defined by the selections $M_R > 400$ GeV and $R^2 > 0.15$. The p_T of the electron (muon) is required to be larger than 25 (20) GeV. To suppress backgrounds from the $W(\ell\nu) + \text{jets}$ and $t\bar{t}$ processes, we require that the transverse mass M_t formed by the lepton momentum and $\vec{p}_T^{\,\rm miss}$ be larger than 120 GeV.

For events in the Multijet category, the search uses a region defined by the selections $M_R > 500$ GeV and $R^2 > 0.25$ and requires the presence of at least two jets with $p_T > 80$ GeV within $|\eta| < 3.0$, for compatibility with the requirements imposed by the hadronic razor triggers. For QCD multijet background events, the $E_T^{\rm miss}$ arises mainly from mismeasurement of the energy of one of the leading jets. In such cases, the two razor megajets tend to lie in a back-to-back configuration. Therefore, to suppress the QCD multijet background, we require that the azimuthal angle $\Delta\phi_R$ between the two razor megajets be less than 2.8 radians.

Finally, events containing signatures consistent with beam-induced background or anomalous noise in the calorimeters are rejected using dedicated filters [90,91].

VI. BACKGROUND MODELING

The main background processes in the search regions considered are $W(\ell\nu)+\text{jets}$ (with $\ell = e,\ \mu,\ \tau$), $Z(\nu\bar{\nu})+\text{jets}$, $t\bar{t}$, and QCD multijet production. For event categories with zero b-tagged jets, the background is primarily composed of the $W(\ell\nu)+\text{jets}$ and $Z(\nu\bar{\nu})+$ jets processes, while for categories with two or more b-tagged jets, it is dominated by the $t\bar{t}$ process. There are also very small contributions from the production of two or three electroweak bosons and from the production of $t\bar{t}$ in association with a W or Z boson. These contributions are summed and labeled "Other" in Figs. 2–5.

We model the background using two independent methods based on control samples in data with entirely independent sets of systematic assumptions. The first method (A) is based on the use of dedicated control regions that isolate specific background processes in order to control and correct the predictions of the MC simulation. The second method (B) is based on a fit to an assumed functional form for the shape of the observed data distribution in the two-dimensional $M_R - R^2$ plane. These two background predictions are compared and cross-checked against each other in order to significantly enhance the robustness of the background estimate.

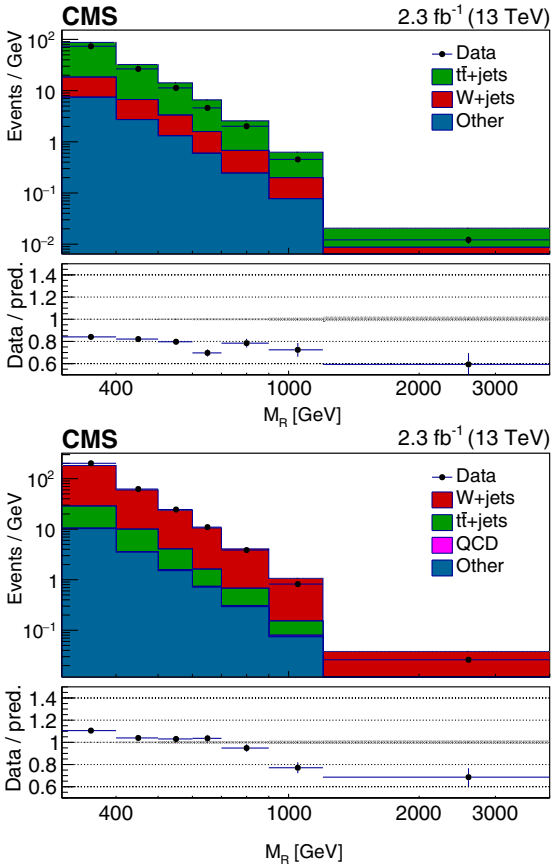

FIG. 2. The M_R distributions for events in the $t\bar{t}$ (left) and $W(\ell\nu)+\text{jets}$ (right) control regions are shown, comparing data with the MC prediction. The ratio of data to the background prediction is shown on the bottom panel, with the statistical uncertainty expressed through the data point error bars and the systematic uncertainty of the background prediction represented by the shaded region. In the right-hand plot, the $t\bar{t}$ MC events have been reweighted according to the corrections derived in the $t\bar{t}$-enhanced control region.

A. Method A: Simulation-assisted background prediction from data

The simulation-assisted method defines dedicated control regions that isolate each of the main background processes. Data in these control regions are used to control and correct the accuracy of the MC prediction for each of the background processes. Corrections for the jet energy response and lepton momentum response are applied to the MC, as are corrections for the trigger efficiency and the selection efficiency of electrons, muons, and b-tagged jets. Any disagreement observed in these control regions is then interpreted as an inaccuracy of the MC in predicting the hadronic recoil spectrum and jet multiplicity. Two alternative formulations of the method are typically used in searches for new physics [25,30,31]. In the first formulation, the data control region yields are extrapolated to the search regions via translation factors derived from simulation. In the second formulation, simulation to data correction factors are derived in bins of the razor variables M_R and R^2 and are then applied to the simulation prediction of the search region yields. The two formulations are identical, and the choice of which formulation is used depends primarily on the convenience of the given data processing sequence. In both cases, the contributions from background processes other than the one under study are subtracted using the MC prediction. We employ the first formulation of the method for the estimate of the QCD background, while the second formulation is used for modeling all other major backgrounds. Details of the control regions used for each of the dominant background processes are described in the subsections below.

Finally, the small contribution from rare background processes such as $t\bar{t}Z$ is modeled using simulation. Systematic uncertainties on the cross sections of these processes are propagated to the final result.

1. $t\bar{t}$ and $W(\ell\nu)+\text{jets}$ background

The control region to isolate the $t\bar{t}$ and $W(\ell\nu)+\text{jets}$ processes is defined by requiring at least one tight electron or muon. To suppress QCD multijet background, the quantities E_T^{miss} and M_T are both required to be larger than 30 GeV. To minimize contamination from potential SUSY processes and to explicitly separate the control region from the search regions, we require $M_T < 100$ GeV. The $t\bar{t}$ enhanced control region is defined by requiring that there be at least one b-tagged jet, and the $W(\ell\nu)+\text{jets}$ enhanced

control region is defined by requiring no such b-tagged jets. Other than these b-tagged jet requirements, we place no explicit requirement on the number of jets in the event, in order to benefit from significantly larger control samples.

We first derive corrections for the $t\bar{t}$ background, and then measure corrections for the $W(\ell\nu)+$ jets process after first applying the corrections already obtained for the $t\bar{t}$ background in the $W(\ell\nu)+$ jets control region. As discussed above, the corrections to the MC prediction are derived in two-dimensional bins of the $M_{\mathrm{R}}-\mathrm{R}^2$ plane. We observe that the M_{R} spectrum predicted by the simulation falls off less steeply than the control region data for both the $t\bar{t}$ and $W(\ell\nu)+$ jets processes, as shown in Fig. 2. In Fig. 3, we show the two dimensional $M_{\mathrm{R}}-\mathrm{R}^2$ distributions for

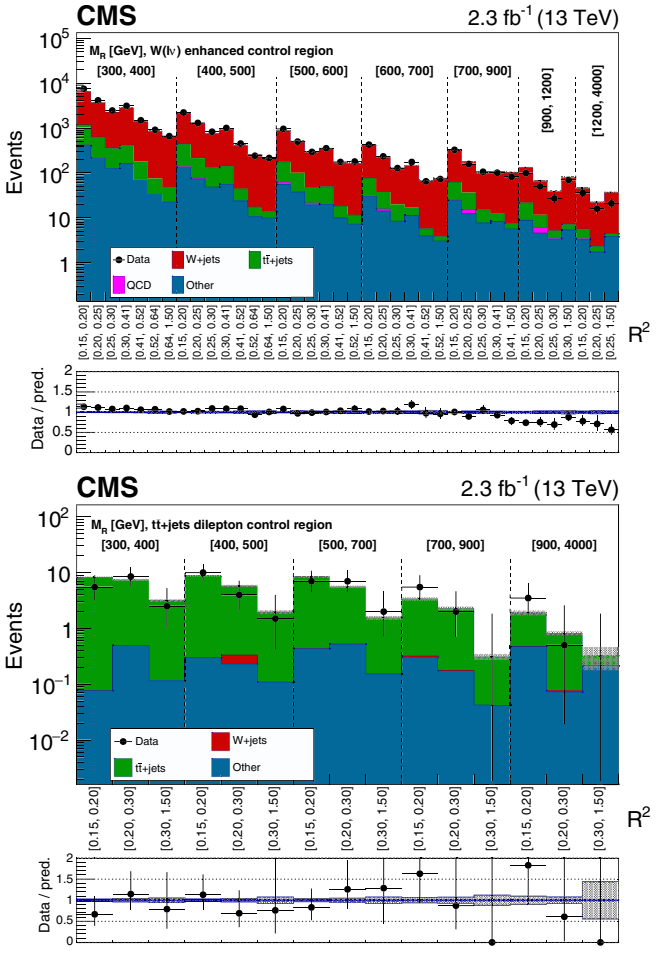

FIG. 3. The two-dimensional $M_{\mathrm{R}}-\mathrm{R}^2$ distribution for the $W(\ell\nu)+$ jets enhanced (upper) and the $t\bar{t}$ dilepton (lower) control regions are shown, comparing data with the MC prediction. The $t\bar{t}$ MC events have been reweighted according to the correction factors derived in the $t\bar{t}$-enhanced control region. The two-dimensional $M_{\mathrm{R}}-\mathrm{R}^2$ distribution is shown in a one dimensional representation, with each M_{R} bin marked by the dashed lines and labeled near the top and each R^2 bin labeled below. The bottom panel shows the ratio of data to the background prediction, with uncertainties displayed as in Fig. 2.

data and simulation in the $W(\ell\nu)+$ jets control region. The statistical uncertainties in the correction factors due to limited event yields in the control region bins are propagated and dominate the total uncertainty of the background prediction. For bins at large M_{R} (near 1000 GeV), the statistical uncertainties range between 15% and 50%.

Corrections to the MC simulation are first measured and applied as a function of M_{R} and R^2, inclusively in the number of selected jets. As our search region requires a higher multiplicity of jets, an additional correction factor is required to accurately model the jet multiplicity. We measure this additional correction factor to be 0.90 ± 0.03 by comparing the data and the MC prediction in the $W(\ell\nu)+$ jets and $t\bar{t}$ control region for events with four or more jets. To control for possible simulation mismodeling that is correlated between the number of jets and the razor variables, we perform additional cross-checks of the M_{R} and R^2 distributions in bins of the number of b-tagged jets in the $t\bar{t}$ and $W(\ell\nu)+$ jets control regions for events with four or more jets. For bins that show statistically significant disagreement, the size of the disagreement is propagated as a systematic uncertainty. The typical range of these additional systematic uncertainties is between 10% and 30%.

The $t\bar{t}$ and $W(\ell\nu)+$ jets backgrounds in the zero-lepton Multijet event category are composed of lost lepton events with at least one lepton in the final state, which is either out of acceptance or fails the veto electron, veto muon, or τ_{h} selection. To ensure a good understanding of the rate of lost lepton events in data and the MC simulation, two additional control regions are defined to evaluate the accuracy of the modeling of the acceptance and efficiency for selecting veto electrons, veto muons, or τ_{h}. We require events in the veto lepton (τ_{h} candidate) control region to have at least one veto electron or muon (τ_{h} candidate) selected. The M_{T} is required to be between 30 and 100 GeV in order to suppress QCD multijet background and contamination from potential new physics processes. At least two jets with $p_{\mathrm{T}}>80$ GeV and at least four jets with $p_{\mathrm{T}}>40$ GeV are required, consistent with the search region requirements. Finally, we consider events with $M_{\mathrm{R}}>400$ GeV and $\mathrm{R}^2>0.25$. The distribution of the veto lepton p_{T} for events in the veto lepton and veto τ_{h} control regions are shown in Fig. 4 and demonstrate that the MC models describe well the observed data. The observed discrepancies in any bin are propagated as systematic uncertainties in the prediction of the $t\bar{t}$ and $W(\ell\nu)+$ jets backgrounds in the Multijet category search region.

The $t\bar{t}$ background in the Electron and Muon Multijet categories is primarily from the dilepton decay mode as the M_t requirement highly suppresses the semileptonic decay mode. Corrections to the MC simulation derived from the $t\bar{t}$ control region primarily arise from semileptonic decays. We define an additional control region enhanced in dilepton $t\bar{t}$ decays to confirm that the MC corrections derived from a

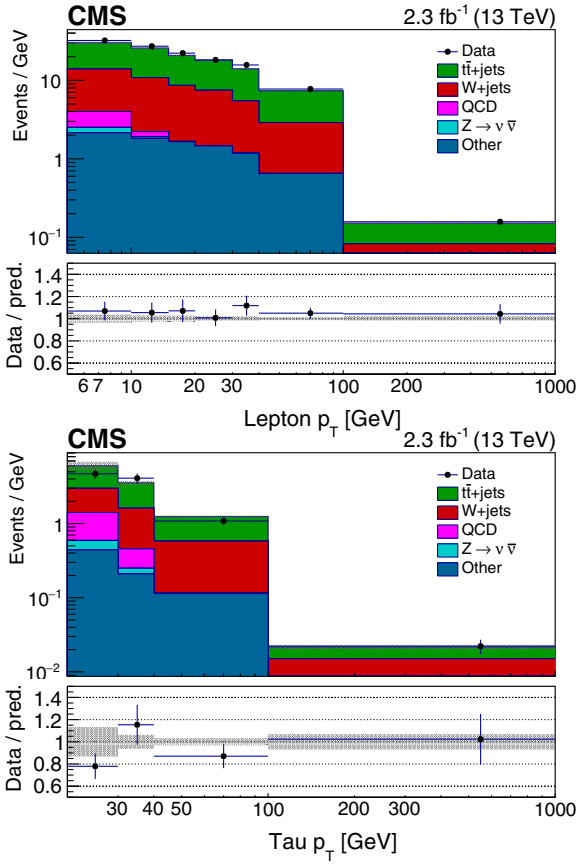

FIG. 4. The p_{T} distributions of the veto electron or muon (left) and the veto τ_{h} (right) is shown for events in the veto lepton control regions, comparing data with the MC prediction. The $t\bar{t}$ and $W(\ell\nu)+$jets MC events have been reweighted according to the correction factors derived in the $t\bar{t}$ enhanced and $W(\ell\nu)+$jets enhanced control regions, respectively. The bottom panel shows the ratio of data to the background prediction, with uncertainties displayed as in Fig. 2.

region dominated by semileptonic decays also apply to dilepton decays. We select events with two tight leptons, both with $p_{\mathrm{T}} > 30$ GeV, $E_{\mathrm{T}}^{\mathrm{miss}} > 40$ GeV, and dilepton mass larger than 20 GeV. For events with two leptons of the same flavor, we additionally veto events with a dilepton mass between 76 and 106 GeV in order to suppress background from Z boson decays. At least one b-tagged jet is required to enhance the purity for the $t\bar{t}$ process. Finally, we mimic the phase space region similar to our search region in the Electron and Muon Multijet categories by treating one lepton as having failed the identification criteria and applying the M_{T} requirement using the other lepton. The correction factors measured in the $t\bar{t}$ control region are applied to the MC prediction of the dilepton $t\bar{t}$ cross-check region in bins of M_{R} and R^2. In Fig. 3, we show the $M_{\mathrm{R}} - \mathrm{R}^2$ distribution for the dilepton $t\bar{t}$ cross-check region in events with four or more jets, and we observe no significant mismodeling by the simulation, indicating that the measured corrections are accurate.

2. $Z \to \nu\bar{\nu}$ background

Three independent control regions are used to predict the $Z(\nu\bar{\nu})+$jets background, relying on the assumption that Monte Carlo simulation mismodeling of the hadronic recoil spectrum and the jet multiplicity distribution of the $Z(\nu\bar{\nu})+$jets process are similar to those of the $W(\ell\nu)+$jets and $\gamma+$jets processes. The primary and most populated control region is the $\gamma+$jets control region, defined by selecting events with at least one photon passing loose identification and isolation requirements. The events are triggered using single-photon triggers, and the photon is required to have $p_t > 50$ GeV. The momentum of the photon candidate in the transverse plane is added vectorially to $\vec{p}_{\mathrm{T}}^{\mathrm{miss}}$ in order to simulate an invisible particle, as one would have in the case of a $\mathrm{Z} \to \nu\bar{\nu}$ decay, and the M_{R} and R^2 variables are computed according to this invisible decay scenario. A template fit to the distribution of $\sigma_{\eta\eta}$ is performed to determine the contribution from misidentified photons to the $\gamma+$jets control region, and this is found to be about 5%, independent of M_{R} and R^2. Events from the $\gamma+$jets process where the photon is produced within the cone of a jet (labeled as $\gamma+$jets fragmentation) are considered to be background and subtracted using the MC prediction. Backgrounds from rarer processes such as $W\gamma$, $Z\gamma$, and $t\bar{t}\gamma$ are also subtracted. In Fig. 5, we show the M_{R} distribution as well as the two-dimensional $M_{\mathrm{R}} - \mathrm{R}^2$ distribution for the $\gamma+$jets control region, where we again observe a steeper M_{R} falloff in the data compared to the simulation. Correction factors are derived in bins of M_{R} and R^2 and applied to the MC prediction for the $Z \to \nu\bar{\nu}$ background in the search region. The statistical uncertainties for the correction factors range between 10% and 30% and are among the dominant uncertainties for the $Z \to \nu\bar{\nu}$ background prediction. Analogously to the procedure for the $t\bar{t}$ and $W(\ell\nu)+$jets control region, we derive an additional correction factor of 0.87 ± 0.05 to accurately describe the yield in events with four or more jets. Additional cross-checks are performed in bins of the number of b-tagged jets, and systematic uncertainties ranging from 4% for events with zero b-tagged jets to 58% for events with three or more b-tagged jets are derived.

The second control region, enhanced in the $W(\ell\nu)+$jets process, is defined identically to the $W(\ell\nu)+$jets control region described in Sec. VI A 1, except that the lepton is treated as invisible by adding its momentum vectorially to $\vec{p}_{\mathrm{T}}^{\mathrm{miss}}$, and the M_{R} and R^2 variables are computed accordingly. Correction factors computed using events from this control region are compared to those computed from the $\gamma+$jets control region and exhibit differences ranging between 10% and 40% depending on the $M_{\mathrm{R}} - \mathrm{R}^2$ bin.

These differences are propagated as a systematic uncertainty. The third control region, enhanced in $Z \to \ell^+\ell^-$ decays, is defined by selecting events with two tight electrons or two tight muons and requiring that the dilepton

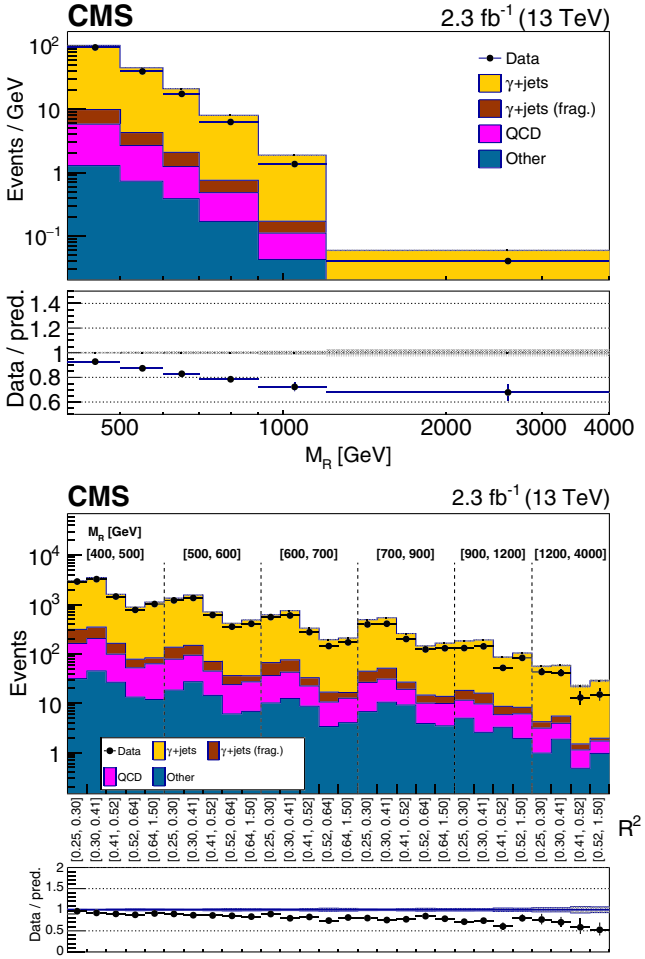

FIG. 5. The one-dimensional distribution of M_R in the $\gamma +$ jets control region (above) and the two-dimensional $M_R - R^2$ distribution in the $\gamma +$ jets control region (below) are shown. The two-dimensional $M_R - R^2$ distribution is shown in a one-dimensional representation as in Fig. 3. The bottom panel shows the ratio of data to the background prediction, with uncertainties displayed as in Fig. 2.

mass is between 76 and 106 GeV. Events are required to have no b-tagged jets in order to suppress $t\bar{t}$ background. The two leptons are treated as invisible by adding their momenta vectorially to $\vec{p}_T^{\,\text{miss}}$. We apply the correction factors obtained from the $\gamma +$ jet control region to the $Z \to \ell^+\ell^-$ MC prediction and perform a cross-check against data in this control region. No significant discrepancy between the data and the prediction is observed.

3. QCD multijet background

The QCD multijet processes contribute about 10% of the total background in the zero-lepton Multijet event category for bins with zero or one b-tagged jet. Such events enter the search regions in the tails of the E_T^{miss} distribution when the energy of one of the jets in the event is significantly under- or overmeasured. In most such situations, the $\vec{p}_T^{\,\text{miss}}$ points either toward or away from the leading jets, and therefore the two megajets tend to be in a back-to-back configuration. The search region is defined by requiring that the azimuthal angle between the two megajets $\Delta\phi_R$ be less than 2.8, which was found to be an optimal selection based on studies of QCD multijet and signal simulated samples. We define the control region for the QCD background process to be events with $\Delta\phi_R > 2.8$, keeping all other selection requirements identical to those for the search region. The purity of the QCD multijet process in the control region is more than 70%.

After subtracting the non-QCD background, we project the observed data yield in the control region to the search region using the translation factor ζ,

$$\zeta = \frac{N(|\Delta\phi_R| < 2.8)}{N(|\Delta\phi_R| > 2.8)}, \tag{5}$$

where the numerator and denominator are the number of events passing and failing the selection on $|\Delta\phi_R| < 2.8$, respectively. We find that the translation factor calculated from the MC simulation decreases as a function of M_R and is, to a large degree, constant as a function of R^2. Using data events in the low R^2 region (0.15 to 0.25), dominated by QCD multijet background, we measure the translation factor ζ as a function of M_R to cross-check the values obtained from the simulation. The M_R dependence of ζ is modeled as the sum of a power law and a constant. This functional shape is fitted to the values of ζ calculated from the MC. A systematic uncertainty of 87% is propagated, covering both the spread around the fitted model as a function of M_R and R^2 in simulation and the difference between the values measured in simulation and data. The function used for ζ and the values measured in data and simulation are shown in Fig. 6.

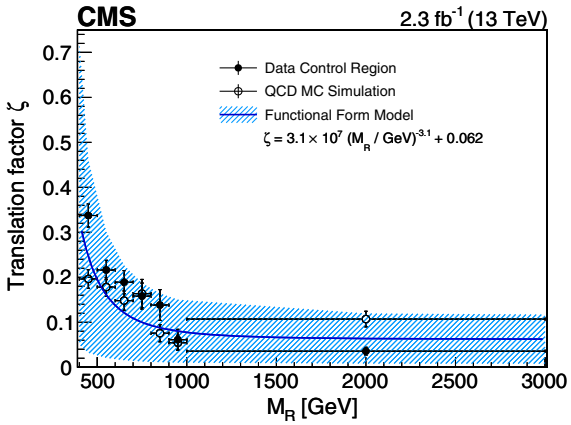

FIG. 6. The translation factor ζ is shown as a function of M_R. The curve shows the functional form used to model the M_R dependence, and the open circle and black dot data points are the values of ζ measured in the low-R^2 data control region and the QCD MC simulation, respectively. The hashed region indicates the size of the systematic uncertainty in ζ.

We perform two additional cross-checks on the accuracy of the MC prediction for ζ in control regions dominated by processes similar to the QCD multijet background with no invisible neutrinos in the final state. The first cross-check is performed on a dimuon control region enhanced in $Z \to \mu^+\mu^-$ decays, and the second cross-check is performed on a dijet control region enhanced in QCD dijet events. In both cases, the events at large R^2 result from cases similar to our search region where the energy of a leading jet is severely mismeasured. We compare the values of ζ measured in these data control regions to the values predicted by the simulation and observe agreement within 20%, well within the systematic uncertainty of 87% assigned to the QCD background estimate.

B. Method B: Fit-based background prediction

The second background prediction method is based on a fit to the data with an assumed functional form for the shape of the background distribution in the $M_R - R^2$ plane. Based on past studies [54,56], the shape of the background in the M_R and R^2 variables is found to be well described by the following functional form,

$$f_{SM}(M_R, R^2) = [b(M_R - M_R^0)^{1/n}(R^2 - R_0^2)^{1/n} - 1] \times e^{-bn(M_R - M_R^0)^{1/n}(R^2 - R_0^2)^{1/n}}, \quad (6)$$

where M_R^0, R_0^2, b, and n are free parameters. In the original study [54], this function with n fixed to 1 was used to model the data in each category. The function choice was motivated by the observation that for $n = 1$ the function projects to an exponential both on R^2 and M_R, and b is proportional to the exponential rate parameter in each one-dimensional projection. The generalized function in Eq. (6) was found to be in better agreement with the SM backgrounds over a larger range of R^2 and M_R [56] in comparison to the choice with n fixed to 1. The two parameters b and n determine the tail of the distribution in the two-dimensional plane, while the M_R^0 (R_0^2) parameter affects the tail of the one-dimensional projection on R^2 (M_R).

The background estimation is performed using an extended, binned, maximum likelihood fit to the M_R and R^2 distribution in one of two ways:

(i) A fit to the data in the sideband regions in M_R and R^2, defined more precisely below, as a model-independent way to look for excesses or discrepancies. The fit is performed using only the data in the sideband, and the functional form is extrapolated to the full M_R and R^2 plane.

(ii) A fit to the data in the full search region in M_R and R^2 under background-only and signal-plus-background hypotheses, following a modified frequentist approach (LHC CL_s) [92–96] to interpret the data in the context of particular SUSY simplified models.

The sideband region is defined to be 100 GeV in width in M_R and 0.05 in R^2. Explicitly, for the Multijet event category, it comprises the region $500\,\text{GeV} < M_R < 600\,\text{GeV}$ and $R^2 > 0.3$, plus the region $M_R > 500$ GeV and $0.25 < R^2 < 0.3$. For the Muon and Electron Multijet event categories, it comprises the region 400 GeV $< M_R <$ 500 GeV and $R^2 > 0.2$, plus the region $M_R > 400$ GeV and $0.15 < R^2 < 0.2$.

For each event category, we fit the two-dimensional distribution of M_R and R^2 in the sideband region using the above functional form, separately for events with zero, one, two, and three or more b-tagged jets. The normalization in each event category and each b-tagged jet bin is independently varied in the fit. Due to the lack of data events in the category with three or more b-tagged jets, we constrain the shape in this category to be related to the shape for events with two b-tagged jets as follows,

$$f_{SM}^{\geq 3b}(M_R, R^2) = (1 + m_{M_R}(M_R - M_R^{\text{offset}}))f_{SM}^{2b}(M_R, R^2), \quad (7)$$

where $f_{SM}^{2b}(M_R, R^2)$ and $f_{SM}^{\geq 3b}(M_R, R^2)$ are the probability density functions for events with two and with three or more b-tagged jets, respectively; M_R^{offset} is the lowest M_R value in a particular event category; and m_{M_R} is a floating parameter constrained by a Gaussian distribution centered at the value measured using the simulation and with a 100% uncertainty. The above form for the shape of the background events with three or more b-tagged jets is verified in simulation.

Numerous tests are performed to establish the robustness of the fit model in adequately describing the underlying distributions. To demonstrate that the background model gives an accurate description of the background distributions, we construct a representative data set using MC samples and perform the background fit using the form given by Eq. (6). Goodness of fit is evaluated by comparing the background prediction from the fit with the prediction from the simulation. This procedure is performed separately for each of the search categories, and we find that the fit function yields an accurate representation of the background predicted by the simulation.

We also observe that the accuracy of the fit model is insensitive to variations of the background composition predicted by the simulation in each event category by altering relative contributions of the dominant backgrounds, performing a new fit with the alternative background composition, and comparing the new fit results to the nominal fit result. The contributions of the main $t\bar{t}$, $W(\ell\nu)$ + jets, and $Z(\nu\bar{\nu})$ backgrounds are varied by 30%, and the rare backgrounds from QCD multijet and $t\bar{t}Z$ processes are varied by 100%. For the Muon and Electron Multijet event categories, we also vary the contributions from the dileptonic and semileptonic decays of the $t\bar{t}$

background separately by 30%. In each of these tests, we observe that the chosen functional form can adequately describe the shapes of the M_R and R^2 distributions as predicted by the modified MC simulation.

Additional pseudoexperiment studies are performed comparing the background prediction from the sideband fit and the full region fit to evaluate the average deviation between the two fit predictions. We observe that the sideband fit and the full region fit predictions in the signal-sensitive region differ by up to 15%, and we propagate an additional systematic uncertainty to the sideband fit background prediction to cover this average difference.

To illustrate method B, we present the data and fit-based background predictions in Fig. 7, for events in the two b-tag and three or more b-tag Multijet categories. The number of events observed in data is compared to the prediction from the sideband fit in the M_R and R^2 bins. To quantify the agreement between the background model and the observation, we generate alternative sets of background shape parameters from the covariance matrix calculated by the fit.

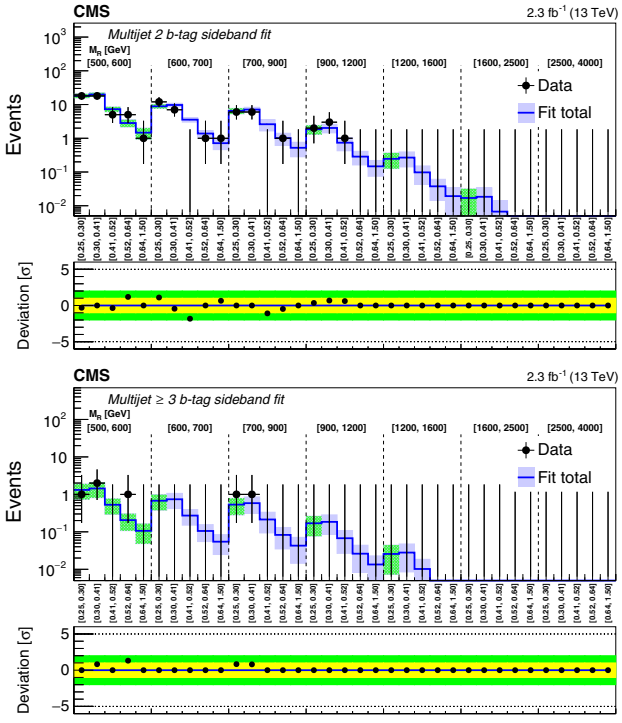

FIG. 7. Comparison of the sideband fit background prediction with the observed data in bins of M_R and R^2 variables in the Multijet category for the 2 b-tag (upper) and ≥ 3 b-tag (lower) bins. Vertical dashed lines denote the boundaries of different M_R bins. On the upper panels, the colored bands represent the systematic uncertainties in the background prediction, and the uncertainty bands for the sideband bins are shown in green. On the bottom panels, the deviations between the observed data and the background prediction are plotted in units of standard deviation (σ), taking into account both statistical and systematic uncertainties. The green and yellow horizontal bands show the boundaries of 1 and 2σ.

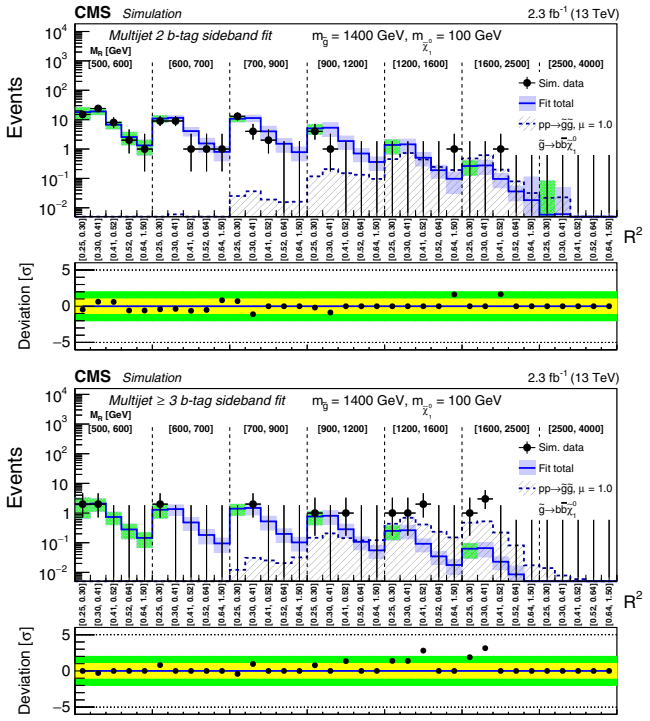

FIG. 8. The result of the background-only fit performed in the sideband of the 2 b-tag (upper) and ≥ 3 b-tag (lower) bins of the Multijet category on a signal-plus-background pseudodata set assuming a gluino pair production simplified model signal, where gluinos decay with a 100% branching fraction to a $b\bar{b}$ pair and the LSP, with $m_{\tilde{g}} = 1.4$ TeV and $m_{\tilde{\chi}_1^0} = 100$ GeV, at nominal signal strength. A detailed explanation of the figure format is given in the caption of Fig. 7.

An ensemble of pseudoexperiment data sets is created, generating random (M_R, R^2) pairs distributed according to each of these alternative shapes. For each $M_R - R^2$ bin, the distribution of the predicted yields from the ensemble of pseudoexperiments is compared to the observed yield in data. The agreement between the predicted and the observed yields is described as a two-sided p-value and translated into the corresponding number of standard deviations for a normal distribution. Positive (negative) significance indicates the observed yield is larger (smaller) than the predicted one. We find that the pattern of differences between data and background predictions in the different bins considered is consistent with statistical fluctuations.

To demonstrate that the model-independent sideband fit procedure used in the analysis would be sensitive to the presence of a signal, we perform a signal injection test. We sample a signal-plus-background pseudodata set and perform a background-only fit in the sideband. We show one illustrative example of such a test in Fig. 8, where we inject a signal corresponding to gluino pair production, in which each gluino decays to a neutralino and a $b\bar{b}$ pair with $m_{\tilde{g}} = 1.4$ TeV and $m_{\tilde{\chi}_1^0} = 100$ GeV. The deviations with respect to the fit predictions are shown for the two b-tag and three

or more b-tag Multijet categories. We observe characteristic patterns of excesses in two adjacent groups of bins neighboring in M_R.

C. Comparison of two methods

The background predictions obtained from methods A and B are systematically compared in all of the search region categories. For method B, the model-independent fit to the sideband is used for this comparison. In Fig. 9, we show the comparison of the two background predictions for two example event categories. The predictions from the two methods agree within the uncertainties of each method. The uncertainty from the fit-based method tends to be slightly larger at high M_R and R^2 due to the additional uncertainty in the exact shape of the tail of the distribution, as the n and b parameters are not strongly constrained by the sideband data.

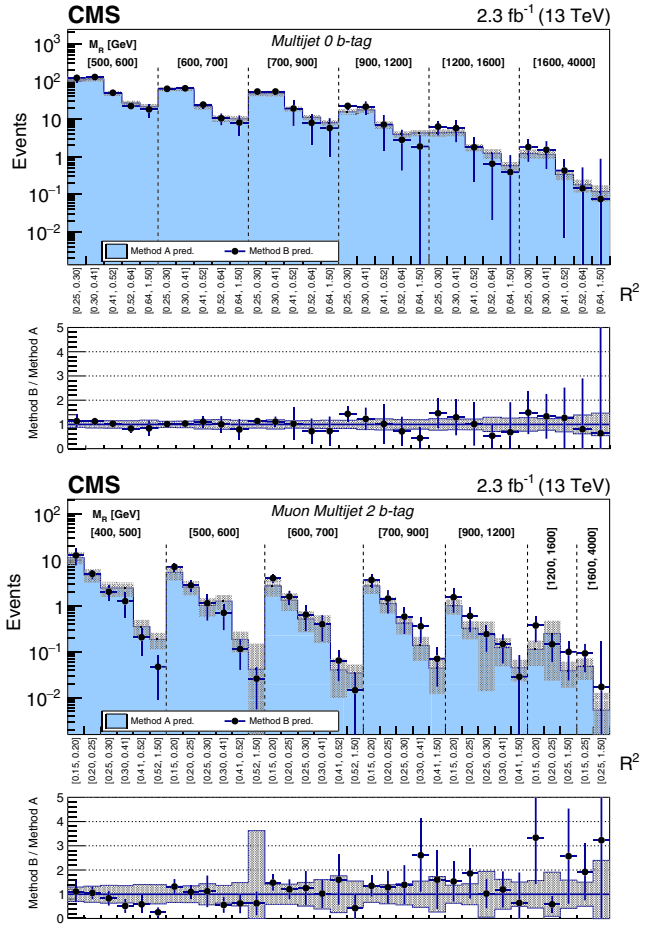

FIG. 9. Comparisons of the two alternative background predictions for the $M_R - R^2$ distribution for the zero b-tag bin of the Multijet category (upper) and the 2 b-tag bin of the Muon Multijet category (lower). The two-dimensional $M_R - R^2$ distribution is shown in a one-dimensional representation, with each M_R bin marked by the dashed lines and labeled near the top and each R^2 bin labeled below. The ratios of the method B fit-based predictions to the method A simulation-assisted predictions are shown on the bottom panels. The method B uncertainty is represented by the error bars on the data points, and the method A uncertainty is represented by the shaded region.

The two background predictions use methods based on data that make very different systematic assumptions. Method A assumes that corrections to the simulation prediction measured in control regions apply also to the signal regions, while method B assumes that the shape of the background distribution in M_R and R^2 is well described by a particular exponentially falling functional form. The agreement observed between predictions obtained using these two very different methods significantly enhances the confidence of the background modeling and also validates the respective assumptions.

VII. SYSTEMATIC UNCERTAINTIES

Various systematic uncertainties are considered in the evaluation of the signal and background predictions. Different types of systematic uncertainties are considered for the two different background models.

For method A, the largest uncertainties arise from the precision with which the MC corrections are measured. The dominant uncertainties in the correction factors result from statistical uncertainties due to the limited size of the control region event sample. We also propagate systematic uncertainties in the theoretical cross section for the small residual backgrounds present in the control regions, and they contribute 2%–5% to the correction factor uncertainty. Additional systematic uncertainties are computed from the procedure that tests that the accuracy of the MC corrections as a function of (M_R, R^2) and the number of b-tagged jets in events with four or more jets. The total uncertainty from this procedure ranges from 10% for the most populated bins to 50% and 100% for the least populated bins. For the $Z \to \nu\bar{\nu}$ process, we also propagate

TABLE I. Summary of the main instrumental and theoretical systematic uncertainties. The systematic uncertainty associated to the modeling of the initial-state radiation is only applied for events with recoil above 400 GeV.

Source	On signal and/or bkg	Typical values (%)
Jet energy scale	Both	2–15
Electron energy scale	Both	7–9
Muon momentum scale	Both	7–9
Muon efficiency	Both	7–8
Electron efficiency	Both	7–8
Trigger efficiency	Both	3
b-tagging efficiency	Both	6–15
b-mistagging efficiency	Both	4–7
Missing higher orders	Both	10–25
Integrated luminosity	Both	2.7
Fast simulation corrections	Signal only	0–10
Initial-state radiation	Signal only	15–30

the difference in the correction factors measured in the three alternative control regions as a systematic uncertainty, intended to estimate the possible differences in the simulation mismodeling of the hadronic recoil for the $\gamma+$jets process and the $Z(\nu\bar{\nu})+$jets process. These systematic uncertainties range from 10% to 40%. For the QCD multijet background prediction, the statistical uncertainty due to limited event counts in the $\Delta\phi_{\mathrm{R}} > 2.8$ control regions and the systematic uncertainty of 87% in the translation factor ζ are propagated.

For method B, the systematic uncertainties in the background are propagated as part of the maximum likelihood fit procedure. For each event category, the background shape in M_{R} and R^2 is described by four independent parameters: two that control the exponential falloff and two that control the behavior of the nonexponential tail. Systematic uncertainties in the background are propagated through the freedom of these unconstrained shape parameters in the fit model. For more populated bins, such as the zero b-tag and one b-tag bins in the Multijet category, the systematic uncertainties range from about 30% at low M_{R} and R^2 to about 70% at high M_{R} and R^2. For sparsely populated bins such as the three or more b-tag bin in the Muon Multijet or Electron Multijet categories, the systematic uncertainties range from about 60% at low M_{R} and R^2 to more than 200% at high M_{R} and R^2.

Systematic uncertainties due to instrumental and theoretical effects are propagated as shape uncertainties in the signal predictions for methods A and B and on the background predictions for method A. The background prediction from method B is not affected by these

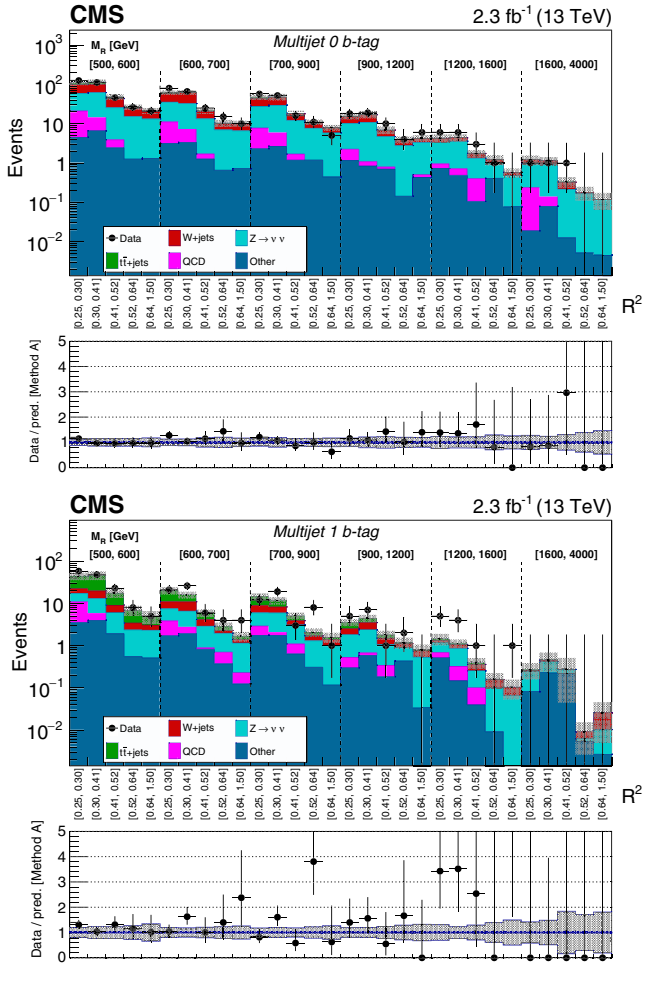

FIG. 10. The M_{R}-R^2 distribution observed in data is shown along with the background prediction obtained from method A for the Multijet event category in the zero b-tag (upper) and 1 b-tag (lower) bins. The two-dimensional M_{R}-R^2 distribution is shown in a one-dimensional representation, with each M_{R} bin marked by the dashed lines and labeled near the top, and each R^2 bin labeled below. The ratio of data to the background prediction is shown on the bottom panels, with the statistical uncertainty expressed through the data point error bars and the systematic uncertainty of the background prediction represented by the shaded region.

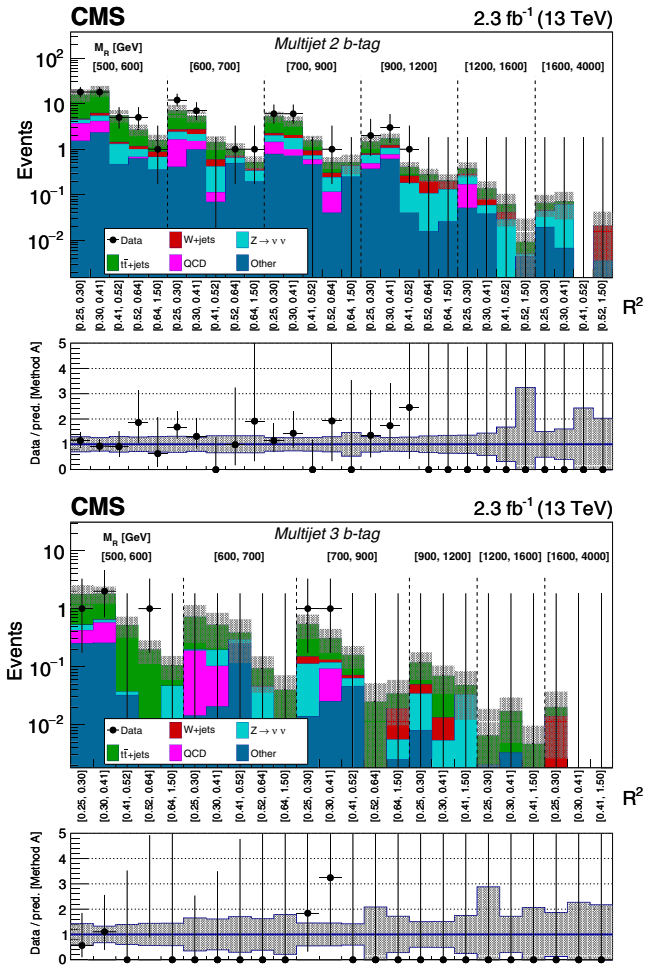

FIG. 11. The M_{R}-R^2 distribution observed in data is shown along with the background prediction obtained from method A for the Multijet event category in the 2 b-tag (upper) and ≥ 3 b-tag (lower) bins. A detailed explanation of the panels is given in the caption of Fig. 10.

uncertainties as the shape and normalization are measured from data. Uncertainties in the trigger and lepton selection efficiency and the integrated luminosity [97] primarily affect the total normalization. Uncertainties in the b-tagging efficiency affect the relative yields between different b-tag categories. The uncertainties from missing higher-order corrections and the uncertainties in the jet energy and lepton momentum scale affect the shapes of the M_R and R^2 distributions.

For the signal predictions, we also propagate systematic uncertainties due to possible inaccuracies of the fast simulation in modeling the lepton selection and b-tagging efficiencies. These uncertainties were evaluated by comparing the $t\bar{t}$ and signal GEANT-based MC samples with those that used fast simulation. Finally, we propagate an uncertainty in the modeling of initial-state radiation for signal predictions that ranges from 15% for signal events with recoil between 400 and 600 GeV to 30% for events with recoil above 600 GeV. The systematic uncertainties and their typical impact on the background and signal predictions are summarized in Table I.

VIII. RESULTS AND INTERPRETATIONS

We present results of the search using method A as it provides slightly better sensitivity. The two-dimensional M_R-R^2 distributions for the search regions in the Multijet, Electron Multijet, and Muon Multijet categories observed in data are shown in Figs. 10–15, along with the background prediction from method A. We observe no statistically significant discrepancies and interpret the null search result using method A by determining the 95% confidence level (C.L.) upper limits on the production cross sections of the SUSY models presented in Sec. I using a global likelihood determined by combining the likelihoods of the different search boxes and sidebands. Following the LHC CL_s procedure [96], we use the profile likelihood ratio

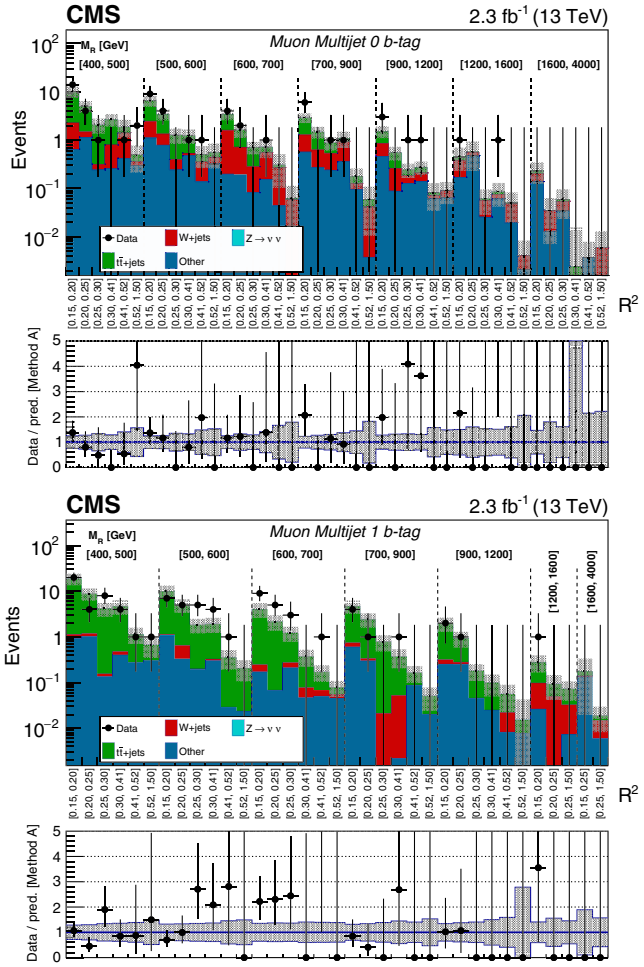

FIG. 12. The M_R-R^2 distribution observed in data is shown along with the background prediction obtained from method A for the Muon Multijet event category in the zero b-tag (upper) and 1 b-tag (lower) bins. A detailed explanation of the panels is given in the caption of Fig. 10.

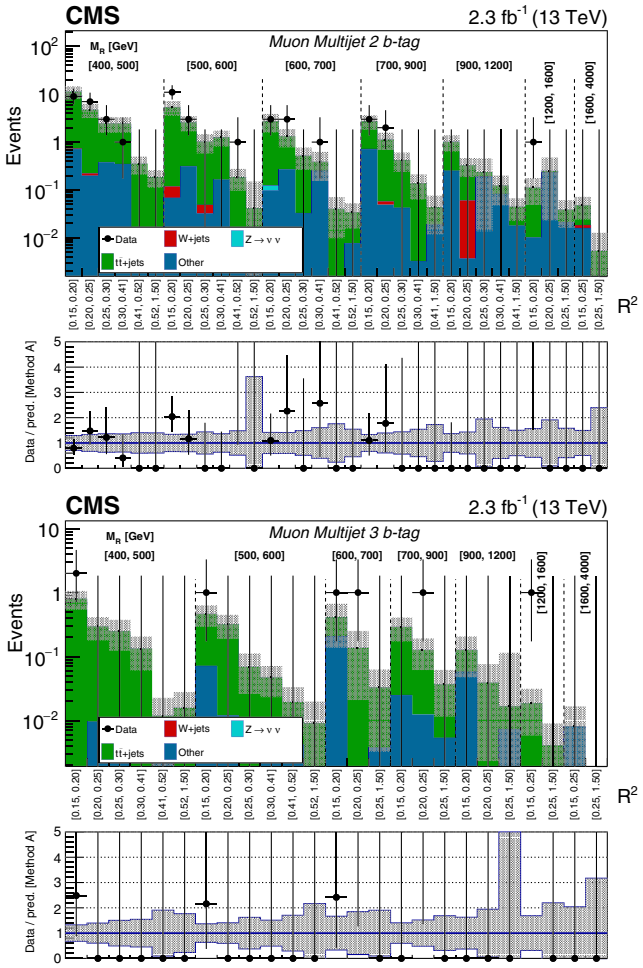

FIG. 13. The M_R-R^2 distribution observed in data is shown along with the background prediction obtained from method A for the Muon Multijet event category in the 2 b-tag (upper) and ≥ 3 b-tag (lower) bins. A detailed explanation of the panels is given in the caption of Fig. 10.

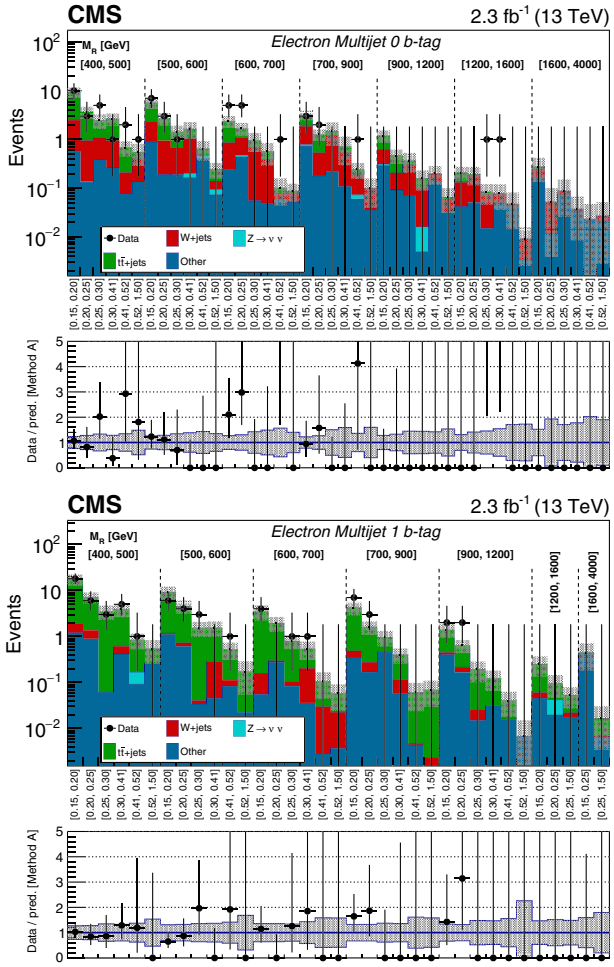

FIG. 14. The M_R-R^2 distribution observed in data is shown along with the background prediction obtained from method A for the Electron Multijet event category in the zero b-tag (upper) and 1 b-tag (lower) bins. A detailed explanation of the panels is given in the caption of Fig. 10.

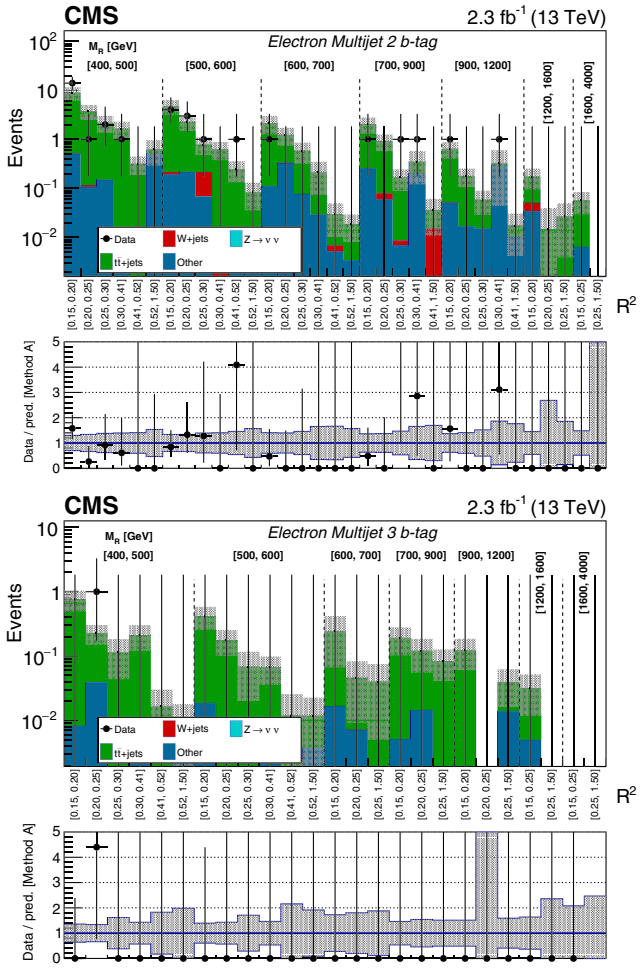

FIG. 15. The M_R-R^2 distribution observed in data is shown along with the background prediction obtained from method A for the Electron Multijet event category in the 2 b-tag (upper) and ≥ 3 b-tag (lower) bins. A detailed explanation of the panels is given in the caption of Fig. 10.

test statistic and the asymptotic formula to evaluate the 95% C.L. observed and expected limits on the SUSY production cross section σ. Systematic uncertainties are taken into account by incorporating nuisance parameters $\boldsymbol{\theta}$, representing different sources of systematic uncertainty, into the likelihood function $L(\sigma, \boldsymbol{\theta})$. For each signal model, the simulated SUSY events are used to estimate the effect of possible signal contamination in the analysis control regions, and the method A background prediction is corrected accordingly. To determine a confidence interval for σ, we construct the profile likelihood ratio test statistic $-2\ln[L(\sigma, \hat{\boldsymbol{\theta}}_\sigma)/L(\hat{\sigma}, \hat{\boldsymbol{\theta}})]$ as a function of σ, where $\hat{\boldsymbol{\theta}}_\sigma$ refers to the conditional maximum likelihood estimators of $\boldsymbol{\theta}$ assuming a given value σ, and $\hat{\sigma}$ and $\hat{\boldsymbol{\theta}}$ correspond to the global maximum of the likelihood. Then, for example, a 68% confidence interval for σ can be taken as the region for which the test statistic is less than 1. By allowing each nuisance parameter to vary, the test statistic curve is wider, reflecting the systematic uncertainty arising from each source and resulting in a larger confidence interval for σ. First, we consider the scenario of gluino pair production decaying to third-generation quarks. Gluino decays to the third generation are enhanced if the masses of the third-generation squarks are significantly lighter than those of the first two generations, a scenario that is strongly motivated in natural SUSY models [61,98–100]. Prompted by this, we consider the three decay modes:

(i) $\tilde{g} \to b\bar{b}\tilde{\chi}^0$,
(ii) $\tilde{g} \to t\bar{t}\tilde{\chi}^0$,
(iii) $\tilde{g} \to b\bar{t}\tilde{\chi}^+{}_1 \to b\bar{t}W^{*+}\tilde{\chi}^0_1$ or the charge conjugate,

where W^* denotes a virtual W boson. Due to a technical limitation inherent in the event generator, we consider these three decay modes for $|m_{\tilde{g}} - m_{\tilde{\chi}^0_1}| \geq 225$ GeV. For $|m_{\tilde{g}} - m_{\tilde{\chi}^0_1}| < 225$ GeV, we only consider the $\tilde{g} \to b\bar{b}\tilde{\chi}^0$ decay mode.

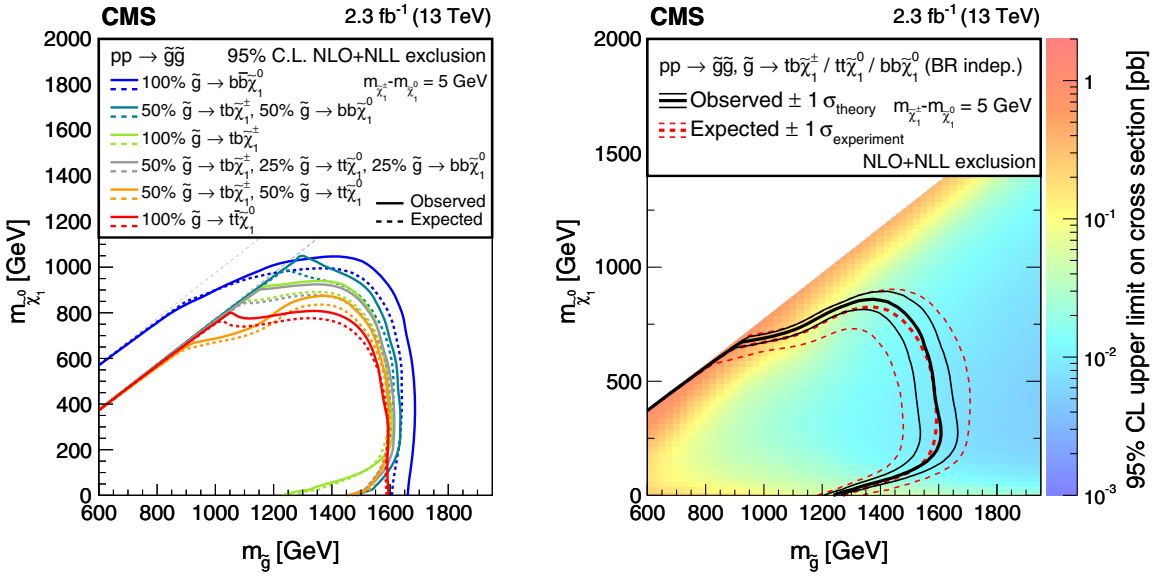

FIG. 16. (Left) the expected and observed 95% C.L. upper limits on the production cross section for gluino pair production decaying to third-generation quarks under various assumptions of the branching fractions. The two gray dashed diagonal lines correspond to $|m_{\tilde{g}} - m_{\tilde{\chi}_1^0}| = 25$ GeV, which is where the scan ends for the $\tilde{g} \to b\bar{b}\tilde{\chi}_1^0$ decay mode, and $|m_{\tilde{g}} - m_{\tilde{\chi}_1^0}| = 225$ GeV, which is where the scan ends for the remaining modes due to a technical limitation inherent in the event generator. For $|m_{\tilde{g}} - m_{\tilde{\chi}_1^0}| < 225$ GeV, we only consider the $\tilde{g} \to b\bar{b}\tilde{\chi}_1^0$ decay mode. (Right) the analogous upper limits on the gluino pair production cross section valid for any values of the gluino decay branching fractions.

The three-body gluino decays considered here capture all of the possible final states within this natural SUSY context including those of two-body gluino decays with intermediate top or bottom squarks. Past studies have shown that LHC searches exhibit a similar sensitivity to three-body and two-body gluino decays with a only a weak dependence on the intermediate squark mass [40].

We perform a scan over all possible branching fractions to these three decay modes and compute limits on the production cross section under each such scenario. The

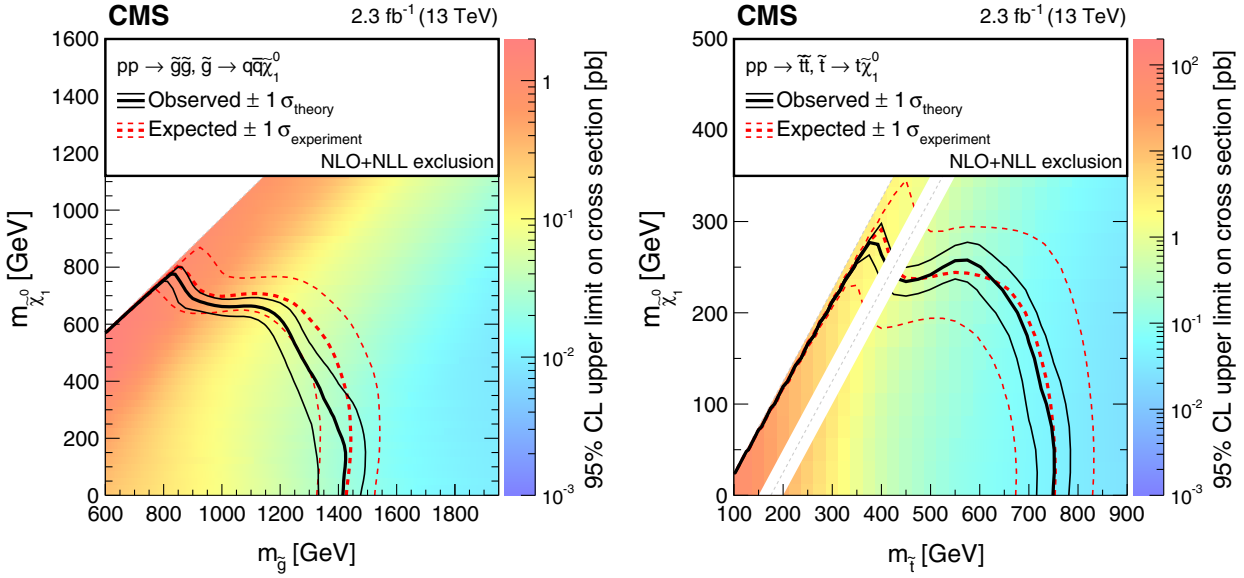

FIG. 17. Expected and observed 95% C.L. upper limits on the production cross section for (left) gluino pair production decaying to two light-flavored quarks and the LSP and (right) top squark pair production decaying to a top quark and the LSP. The white diagonal band in the right plot corresponds to the region $|m_{\tilde{t}} - m_t - m_{\tilde{\chi}_1^0}| < 25$ GeV, where the signal efficiency is a strong function of $m_{\tilde{t}} - m_{\tilde{\chi}_1^0}$, and as a result the precise determination of the cross section upper limit is uncertain because of the finite granularity of the available MC samples in this region of the $(m_{\tilde{t}}, m_{\tilde{\chi}_1^0})$ plane.

production cross section limits for a few characteristic branching fraction scan points are shown on the left of Fig. 16 as a function of the gluino and neutralino masses. We find a range of excluded regions for different branching fraction assumptions and generally observe the strongest limits for the $\tilde{g} \to b\bar{b}\tilde{\chi}_1^0$ decay mode over the full two-dimensional mass plane and the weakest limits for the $\tilde{g} \to t\bar{t}\tilde{\chi}_1^0$ decay mode. For scenarios that include the intermediate decay $\tilde{\chi}_1^+ \to W^{*\pm}\tilde{\chi}_1^0$ and small values of $m_{\tilde{\chi}_1^0}$, the sensitivity is reduced because the LSP carries very little momentum in both the NLSP rest frame and the laboratory frame, resulting in small values of $E_{\mathrm{T}}^{\mathrm{miss}}$ and R^2. By considering the limits obtained for all scanned branching fractions, we calculate the exclusion limits valid for any assumption on the branching fractions, presented on the right of Fig. 16. For an LSP with mass of a few hundred GeV, we exclude pair production of gluinos decaying to third-generation quarks for mass below about 1.6 TeV. This result represents a unique attempt to obtain a branching fraction-independent limit on gluino pair production at the LHC for the scenario in which gluino decays are dominated by three-body decays to third-generation quarks and a neutralino LSP.

In Fig. 17, we present additional interpretations for simplified model scenarios of interest. On the left, we show the production cross section limits on gluino pair production where the gluino decays to two light-flavored quarks and the LSP, and on the right, we show the production cross section limits on top squark pair production where the top squark decays to a top quark and the LSP. For a very light LSP, we exclude top squark production with mass below 750 GeV.

IX. SUMMARY

We have presented an inclusive search for supersymmetry in events with no more than one lepton, a large multiplicity of energetic jets, and missing transverse energy. The search is sensitive to a broad range of SUSY scenarios including the pair production of gluinos and top squarks. The event categorization in the number of leptons and the number of b-tagged jets enhances the search sensitivity for a variety of different SUSY signal scenarios. Two background estimation methods are presented, both based on transfer factors between data control regions and the search regions but having very different systematic assumptions: one relying on the simulation and associated corrections derived in the control regions and the other relying on the accuracy of an assumed functional form for the shape of background distributions in the M_{R} and R^2 variables. The two predictions agree within their uncertainties, thereby demonstrating the robustness of the background modeling.

No significant deviations from the predicted standard model background are observed in any of the search regions, and this result is interpreted in the context of simplified models of gluino or top squark pair production. For top squark decays to a top quark and an LSP with a mass of 100 GeV, we exclude top squarks with masses below 750 GeV. Considering separately the gluino decays to bottom quarks and the LSP or first- and second-generation quarks and the LSP, gluino masses up to 1.65 or 1.4 TeV are excluded, respectively. Furthermore, this search goes beyond the existing simplified model paradigm by interpreting results in a broader context inspired by natural SUSY, with multiple gluino decay modes considered simultaneously. By scanning over all possible branching fractions for three-body gluino decays to third-generation quarks, exclusion limits are derived on gluino pair production that are valid for any values of the gluino decay branching fractions. For a chargino NLSP nearly degenerate in mass with the LSP and LSP masses in the range between 200 and 600 GeV, we exclude gluinos with mass below 1.55 to 1.6 TeV, regardless of their decays. This result is a more generic constraint on gluino production than previously reported at the LHC.

ACKNOWLEDGMENTS

Forschungs-zentren We congratulate our colleagues in the CERN accelerator departments for the excellent performance of the LHC and thank the technical and administrative staffs at CERN and at other CMS institutes for their contributions to the success of the CMS effort. In addition, we gratefully acknowledge the computing centers and personnel of the Worldwide LHC Computing Grid for delivering so effectively the computing infrastructure essential to our analyses. Finally, we acknowledge the enduring support for the construction and operation of the LHC and the CMS detector provided by the following funding agencies: the Austrian Federal Ministry of Science, Research and Economy and the Austrian Science Fund; the Belgian Fonds de la Recherche Scientifique and Fonds voor Wetenschappelijk Onderzoek; the Brazilian Funding Agencies (CNPq, CAPES, FAPERJ, and FAPESP); the Bulgarian Ministry of Education and Science; CERN; the Chinese Academy of Sciences, Ministry of Science and Technology and National Natural Science Foundation of China; the Colombian Funding Agency (COLCIENCIAS); the Croatian Ministry of Science, Education and Sport and the Croatian Science Foundation; the Research Promotion Foundation, Cyprus; the Ministry of Education and Research, Estonian Research Council, via Grants No. IUT23-4 and No. IUT23-6 and European Regional Development Fund, Estonia; the Academy of Finland, Finnish Ministry of Education and Culture, and Helsinki Institute of Physics; the Institut National de Physique Nucléaire et de Physique des Particules/CNRS and Commissariat à l'Énergie Atomique et aux Énergies Alternatives/CEA, France; the Bundesministerium für Bildung und Forschung, Deutsche Forschungsgemeinschaft, and Helmholtz-Gemeinschaft

Deutscher Forschungszentren, Germany; the General Secretariat for Research and Technology, Greece; the National Scientific Research Foundation and National Innovation Office, Hungary; the Department of Atomic Energy and the Department of Science and Technology, India; the Institute for Studies in Theoretical Physics and Mathematics, Iran; the Science Foundation, Ireland; the Istituto Nazionale di Fisica Nucleare, Italy; the Ministry of Science, ICT and Future Planning and National Research Foundation, Republic of Korea; the Lithuanian Academy of Sciences; the Ministry of Education and University of Malaya, Malaysia; the Mexican Funding Agencies (BUAP, CINVESTAV, CONACYT, LNS, SEP, and UASLP-FAI); the Ministry of Business, Innovation and Employment, New Zealand; the Pakistan Atomic Energy Commission; the Ministry of Science and Higher Education and the National Science Centre, Poland; the Fundaćão para a Ciência e a Tecnologia, Portugal; Joint Institute for Nunclear Research in Dubna, the Ministry of Education and Science of the Russian Federation, the Federal Agency of Atomic Energy of the Russian Federation, Russian Academy of Sciences, and the Russian Foundation for Basic Research; the Ministry of Education, Science and Technological Development of Serbia; the Secretaría de Estado de Investigación, Desarrollo e Innovación and Programa Consolider-Ingenio 2010, Spain; the Swiss Funding Agencies (ETH Board, ETH Zurich, PSI, SNF, UniZH, Canton Zurich, and SER); the Ministry of Science and Technology, Taiwan; the Thailand Center of Excellence in Physics, the Institute for the Promotion of Teaching Science and Technology of Thailand, Special Task Force for Activating Research and the National Science and Technology Development Agency of Thailand; the Scientific and Technical Research Council of Turkey and Turkish Atomic Energy Authority; the National Academy of Sciences of Ukraine and State Fund for Fundamental Researches; the Science and Technology Facilities Council, UK; and the US Department of Energy and the US National Science Foundation. Individuals have received support from the Marie-Curie program and the European Research Council and EPLANET, European Union; the Leventis Foundation; the A. P. Sloan Foundation; the Alexander von Humboldt Foundation; the Belgian Federal Science Policy Office; the Fonds pour la Formation à la Recherche dans l'Industrie et dans l'Agriculture, Belgium; the Agentschap voor Innovatie door Wetenschap en Technologie, Belgium; the Ministry of Education, Youth and Sports of the Czech Republic; the Council of Science and Industrial Research, India; the HOMING PLUS program of the Foundation for Polish Science, cofinanced from European Union, Regional Development Fund; the Mobility Plus program of the Ministry of Science and Higher Education, Poland; the OPUS program of the National Science Center, Poland; the Thalis and Aristeia programs cofinanced by EU-ESF and the Greek NSRF; the National Priorities Research Program by Qatar National Research Fund; the Programa Clarín-COFUND del Principado de Asturias; the Rachadapisek Sompot Fund for Postdoctoral Fellowship, Chulalongkorn University, Thailand; the Chulalongkorn Academic into Its 2nd Century Project Advancement Project, Thailand; and the Welch Foundation, Contract No. C-1845.

APPENDIX: RESULTS OF METHOD B FIT-BASED BACKGROUND PREDICTION

In Sec. VI B, we detail the fit-based background prediction methodology and present the model-independent SUSY search results in the two b-tag and three or more b-tag bins of the Multijet category in Fig. 7. In Figs. 18–22 in this Appendix, we present the results of the search for SUSY signal events in the remaining categories, namely the zero b-tag and one b-tag bins of the Multijet, the Muon Multijet, and Electron Multijet categories. No statistically significant deviations from the expected background predictions are observed in these categories in data.

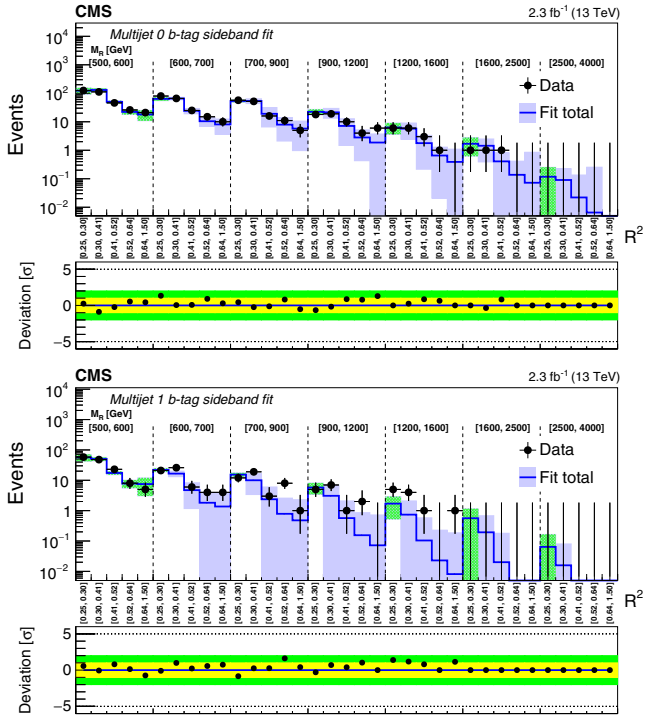

FIG. 18. Comparison of the predicted background with the observed data in bins of M_R and R^2 variables in the Multijet category for the zero b-tag (upper) and 1 b-tag (lower) bins. A detailed explanation of the panels is given in the caption of Fig. 7.

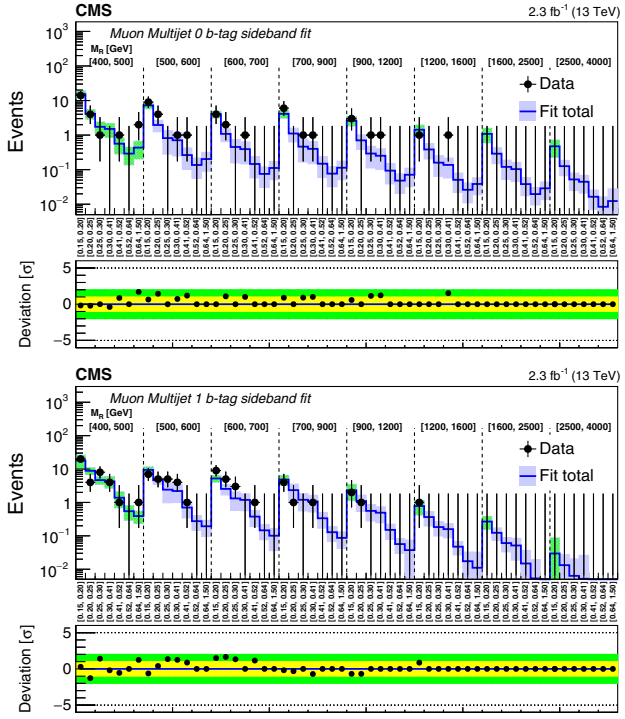

FIG. 19. Comparison of the predicted background with the observed data in bins of M_R and R^2 variables in the Muon Multijet category for the zero b-tag (upper) and 1 b-tag (lower) bins. A detailed explanation of the panels is given in the caption of Fig. 7.

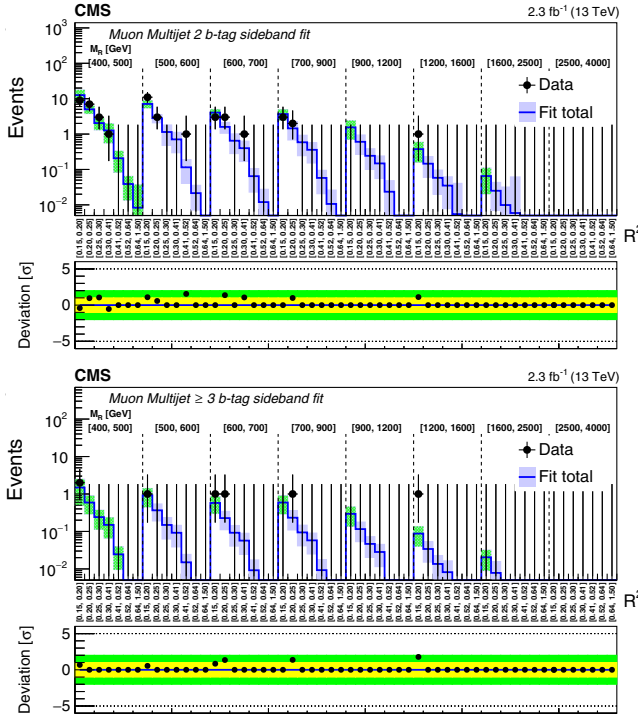

FIG. 20. Comparison of the predicted background with the observed data in bins of M_R and R^2 variables in the Muon Multijet category for the 2 b-tag (upper) and ≥ 3 b-tag (lower) bins. A detailed explanation of the panels is given in the caption of Fig. 7.

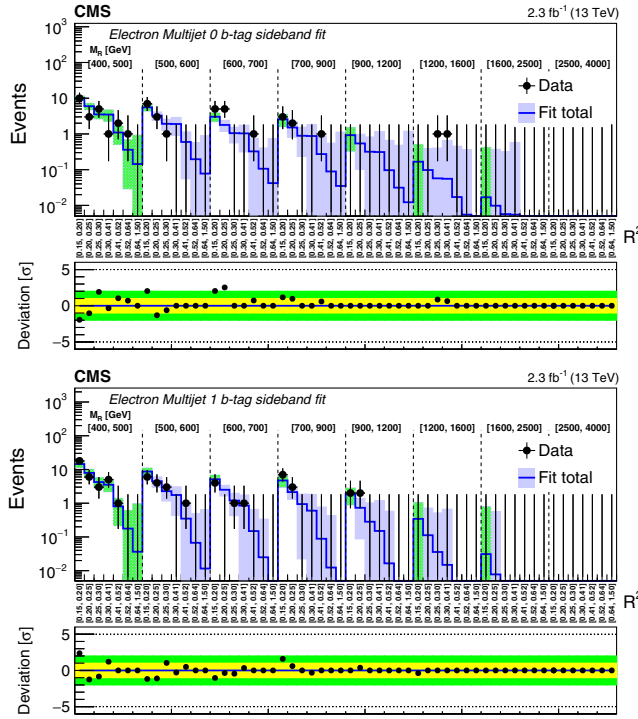

FIG. 21. Comparison of the predicted background with the observed data in bins of M_R and R^2 variables in the Electron Multijet category for the zero b-tag (upper) and 1 b-tag (lower) bins. A detailed explanation of the panels is given in the caption of Fig. 7.

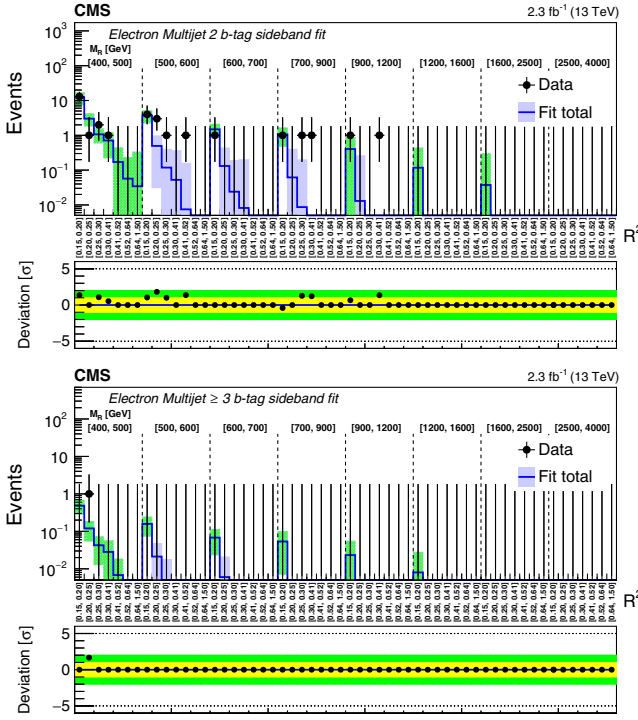

FIG. 22. Comparison of the predicted background with the observed data in bins of M_R and R^2 variables in the Electron Multijet category for the 2 b-tag (upper) and ≥ 3 b-tag (lower) bins. A detailed explanation of the panels is given in the caption of Fig. 7.

[1] J. Wess and B. Zumino, Supergauge transformations in four-dimensions, Nucl. Phys. **B70**, 39 (1974).

[2] Yu. A. Gol'fand and E. P. Likhtman, Extension of the algebra of Poincaré group generators and violation of P invariance, JETP Lett. **13**, 323 (1971).

[3] D. V. Volkov and V. P. Akulov, Possible universal neutrino interaction, JETP Lett. **16**, 438 (1972).

[4] A. H. Chamseddine, Richard L. Arnowitt, and P. Nath, Locally Supersymmetric Grand Unification, Phys. Rev. Lett. **49**, 970 (1982).

[5] G. L. Kane, C. F. Kolda, L. Roszkowski, and J. D. Wells, Study of constrained minimal supersymmetry, Phys. Rev. D **49**, 6173 (1994).

[6] Pierre Fayet, Supergauge invariant extension of the Higgs mechanism and a model for the electron and its neutrino, Nucl. Phys. **B90**, 104 (1975).

[7] R. Barbieri, S. Ferrara, and C. A. Savoy, Gauge models with spontaneously broken local supersymmetry, Phys. Lett. **119B**, 343 (1982).

[8] L. J. Hall, J. D. Lykken, and S. Weinberg, Supergravity as the messenger of supersymmetry breaking, Phys. Rev. D **27**, 2359 (1983).

[9] P. Ramond, Dual theory for free fermions, Phys. Rev. D **3**, 2415 (1971).

[10] E. Witten, Dynamical breaking of supersymmetry, Nucl. Phys. **B188**, 513 (1981).

[11] S. Dimopoulos and H. Georgi, Softly broken supersymmetry and SU(5), Nucl. Phys. **B193**, 150 (1981).

[12] M. Dine, W. Fischler, and M. Srednicki, Supersymmetric technicolor, Grand unification, proceedings, 2nd workshop, Ann Arbor, USA, April 24-26, 1981, Nucl. Phys. **B189**, 575 (1981).

[13] S. Dimopoulos and S. Raby, Supercolor, Nucl. Phys. **B192**, 353 (1981).

[14] N. Sakai, Naturalness in supersymmetric GUTs, Z. Phys. C **11**, 153 (1981).

[15] R. K. Kaul and P. Majumdar, Cancellation of quadratically divergent mass corrections in globally supersymmetric spontaneously broken gauge theories, Nucl. Phys. **B199**, 36 (1982).

[16] S. Dimopoulos, S. Raby, and F. Wilczek, Supersymmetry and the scale of unification, Phys. Rev. D **24**, 1681 (1981).

[17] W. J. Marciano and G. Senjanovic, Predictions of supersymmetric grand unified theories, Phys. Rev. D **25**, 3092 (1982).

[18] M. B. Einhorn and D. R. T. Jones, The weak mixing angle and unification mass in supersymmetric SU(5), Nucl. Phys. **B196**, 475 (1982).

[19] L. E. Ibanez and G. G. Ross, Low-energy predictions in supersymmetric grand unified theories, Phys. Lett. **105B**, 439 (1981).

[20] U. Amaldi, W. de Boer, and H. Furstenau, Comparison of grand unified theories with electroweak and strong coupling constants measured at LEP, Phys. Lett. B **260**, 447 (1991).

[21] P. Langacker and N. Polonsky, The strong coupling, unification, and recent data, Phys. Rev. D **52**, 3081 (1995).

[22] J. R. Ellis, J. S. Hagelin, D. V. Nanopoulos, K. A. Olive, and M. Srednicki, Supersymmetric relics from the Big Bang, Nucl. Phys. **B238**, 453 (1984).

[23] G. Jungman, M. Kamionkowski, and K. Griest, Supersymmetric dark matter, Phys. Rep. **267**, 195 (1996).

[24] CMS Collaboration, Search for top-squark pair production in the single-lepton final state in pp collisions at $\sqrt{s} = 8$ TeV, Eur. Phys. J. C **73**, 2677 (2013).

[25] CMS Collaboration, Search for gluino mediated bottom- and top-squark production in multijet final states in pp collisions at 8 TeV, Phys. Lett. B **725**, 243 (2013).

[26] CMS Collaboration, Search for new physics in the multijet and missing transverse momentum final state in proton-proton collisions at $\sqrt{s} = 8$ TeV, J. High Energy Phys. 06 (2014) 055.

[27] CMS Collaboration, Search for supersymmetry in pp collisions at $\sqrt{s} = 8$ TeV in events with a single lepton, large jet multiplicity, and multiple b jets, Phys. Lett. B **733**, 328 (2014).

[28] CMS Collaboration, Search for new physics in events with same-sign dileptons and jets in pp collisions at $\sqrt{s} = 8$ TeV, J. High Energy Phys. 01 (2014) 163.

[29] CMS Collaboration, Search for supersymmetry in hadronic final states with missing transverse energy using the variables α_t and b-quark multiplicity in pp collisions at 8 TeV, Eur. Phys. J. C **73**, 2568 (2013).

[30] CMS Collaboration, Searches for supersymmetry using the M_{T2} variable in hadronic events produced in pp collisions at 8 TeV, J. High Energy Phys. 05 (2015) 078.

[31] ATLAS Collaboration, Search for new phenomena in final states with large jet multiplicities and missing transverse momentum at $\sqrt{s} = 8$ TeV proton-proton collisions using the ATLAS experiment, J. High Energy Phys. 10 (2013) 130.

[32] ATLAS Collaboration, Search for strong production of supersymmetric particles in final states with missing transverse momentum and at least three b-jets at $\sqrt{s} =$ 8 TeV proton-proton collisions with the ATLAS detector, J. High Energy Phys. 10 (2014) 24.

[33] ATLAS Collaboration, Search for supersymmetry at $\sqrt{s} =$ 8 TeV in final states with jets and two same-sign leptons or three leptons with the ATLAS detector, J. High Energy Phys. 06 (2014) 035.

[34] ATLAS Collaboration, Search for direct pair production of the top squark in all-hadronic final states in proton-proton collisions at $\sqrt{s} = 8$ TeV with the ATLAS detector, J. High Energy Phys. 09 (2014) 015.

[35] ATLAS Collaboration, Search for direct top-squark pair production in final states with two leptons in pp collisions at $\sqrt{s} = 8$ TeV with the ATLAS detector, J. High Energy Phys. 06 (2014) 124.

[36] ATLAS Collaboration, ATLAS Run 1 searches for direct pair production of third-generation squarks at the Large Hadron Collider, Eur. Phys. J. C **75**, 510 (2015).

[37] ATLAS Collaboration, Summary of the searches for squarks and gluinos using $\sqrt{s} = 8$ TeV pp collisions with the ATLAS experiment at the LHC, J. High Energy Phys. 10 (2015) 054.

[38] CMS Collaboration, Search for supersymmetry in the multijet and missing transverse momentum final state in pp collisions at 13 TeV, Phys. Lett. B **758**, 152 (2016).

[39] CMS Collaboration, Search for new physics with the M_{T2} variable in all-jets final states produced in pp collisions at $\sqrt{s} = 13$ TeV, J. High Energy Phys. 10 (2016) 006.

[40] CMS Collaboration, Search for supersymmetry in pp collisions at $\sqrt{s} = 13$ TeV in the single-lepton final state using the sum of masses of large-radius jets, J. High Energy Phys. 09 (2016) 122.

[41] CMS Collaboration, Search for new physics in same-sign dilepton events in proton-proton collisions at $\sqrt{s} = 13$ TeV, Eur. Phys. J. C **76**, 439 (2016).

[42] CMS Collaboration, Search for new physics in final states with two opposite-sign, same-flavor leptons, jets, and missing transverse momentum in pp collisions at $\sqrt{s} = 13$ TeV, arXiv:1607.00915.

[43] ATLAS Collaboration, Search for new phenomena in final states with large jet multiplicities and missing transverse momentum with ATLAS using $\sqrt{s} = 13$ TeV proton-proton collisions, Phys. Lett. B **757**, 334 (2016).

[44] ATLAS Collaboration, Search for supersymmetry at $\sqrt{s} =$ 13 TeV in final states with jets and two same-sign leptons or three leptons with the ATLAS detector, Eur. Phys. J. C **76**, 259 (2016).

[45] ATLAS Collaboration, Search for new phenomena in final states with an energetic jet and large missing transverse momentum in pp collisions at $\sqrt{s} = 13$ TeV using the ATLAS detector, Phys. Rev. D **94**, 032005 (2016).

[46] ATLAS Collaboration, Search for squarks and gluinos in final states with jets and missing transverse momentum at $\sqrt{s} = 13$ TeV with the ATLAS detector, Eur. Phys. J. C **76**, 392 (2016).

[47] ATLAS Collaboration, Search for gluinos in events with an isolated lepton, jets and missing transverse momentum at $\sqrt{s} = 13$ TeV with the ATLAS detector, Eur. Phys. J. C **76**, 565 (2016).

[48] ATLAS Collaboration, Search for pair production of gluinos decaying via stop and sbottom in events with b-jets and large missing transverse momentum in pp collisions at $\sqrt{s} = 13$ TeV with the ATLAS detector, Phys. Rev. D **94**, 032003 (2016).

[49] ATLAS Collaboration, Search for top squarks in final states with one isolated lepton, jets, and missing transverse momentum in $\sqrt{s} = 13$ TeV pp collisions with the ATLAS detector, Phys. Rev. D **94**, 052009 (2016).

[50] ATLAS Collaboration, Search for bottom squark pair production in proton-proton collisions at $\sqrt{s} = 13$ TeV with the ATLAS detector, Eur. Phys. J. C **76**, 547 (2016).

[51] ATLAS Collaboration, Search for supersymmetry in a final state containing two photons and missing transverse momentum in $\sqrt{s} = 13$ TeV pp collisions at the LHC using the ATLAS detector, Eur. Phys. J. C **76**, 517 (2016).

[52] G. R. Farrar and P. Fayet, Phenomenology of the production, decay, and detection of new hadronic states associated with supersymmetry, Phys. Lett. **76B**, 575 (1978).

[53] CMS Collaboration, Inclusive Search for Supersymmetry using the Razor Variables in pp Collisions at $\sqrt{s} = 7$ TeV, Phys. Rev. Lett. **111**, 081802 (2013).

[54] CMS Collaboration, Search for supersymmetry with razor variables in pp collisions at $\sqrt{s} = 7$ TeV, Phys. Rev. D **90**, 112001 (2014).

[55] CMS Collaboration, Inclusive search for squarks and gluinos in pp collisions at $\sqrt{s} = 7$ TeV, Phys. Rev. D **85**, 012004 (2012).

[56] CMS Collaboration, Search for supersymmetry using razor variables in events with b-tagged jets in pp collisions at $\sqrt{s} = 8$ TeV, Phys. Rev. D **91**, 052018 (2015).

[57] CMS Collaboration, Search for supersymmetry in pp collisions at $\sqrt{s} = 8$ TeV in final states with boosted W bosons and b jets using razor variables, Phys. Rev. D **93**, 092009 (2016).

[58] CMS Collaboration, Search for dark matter particles in proton-proton collisions at $\sqrt{s} = 8$ TeV using the razor variables, arXiv:1603.08914.

[59] ATLAS Collaboration, Multi-channel search for squarks and gluinos in $\sqrt{s} = 7$ TeV pp collisions with the ATLAS detector, Eur. Phys. J. C **73**, 2362 (2013).

[60] ATLAS Collaboration, Search for squarks and gluinos in events with isolated leptons, jets and missing transverse momentum at $\sqrt{s} = 8$ TeV with the ATLAS detector, J. High Energy Phys. 04 (2015) 116.

[61] M. Papucci, J. T. Ruderman, and A. Weiler, Natural SUSY endures, J. High Energy Phys. 09 (2012) 035.

[62] CMS Collaboration, The CMS experiment at the CERN LHC, J. Instrum. **3**, S08004 (2008).

[63] J. Alwall, M. Herquet, F. Maltoni, O. Mattelaer, and T. Stelzer, MadGraph5: going beyond, J. High Energy Phys. 06 (2011) 128.

[64] J. Alwall, R. Frederix, S. Frixione, V. Hirschi, F. Maltoni, O. Mattelaer, H.-S. Shao, T. Stelzer, P. Torielli, and M. Zaro, The automated computation of tree-level and next-to-leading order differential cross sections, and their matching to parton shower simulations, J. High Energy Phys. 07 (2014) 079.

[65] S. Alioli, P. Nason, C. Oleari, and E. Re, NLO single-top production matched with shower in POWHEG: s- and t-channel contributions, J. High Energy Phys. 09 (2009) 111; Erratum, J. High Energy Phys.02 (2010) E011.

[66] E. Re, Single-top Wt-channel production matched with parton showers using the POWHEG method, Eur. Phys. J. C **71**, 1547 (2011).

[67] T. Sjöstrand, S. Mrenna, and P. Skands, A brief introduction to PYTHIA 8.1, Comput. Phys. Commun. **178**, 852 (2008).

[68] R. D. Ball *et al.* (NNPDF Collaboration), Parton distributions for the LHC Run II, J. High Energy Phys. 04 (2015) 040.

[69] S. Agostinelli *et al.* (GEANT4 Collaboration), GEANT4—a simulation toolkit, Nucl. Instrum. Methods Phys. Res., Sect. A **506**, 250 (2003).

[70] CMS Collaboration, The fast simulation of the CMS detector at LHC, J. Phys. Conf. Ser. **331**, 032049 (2011).

[71] W. Beenakker, R. Höpker, M. Spira, and P. M. Zerwas, Squark and gluino production at hadron colliders, Nucl. Phys. **B492**, 51 (1997).

[72] A. Kulesza and L. Motyka, Threshold Resummation for Squark-Antisquark and Gluino-Pair Production at the LHC, Phys. Rev. Lett. **102**, 111802 (2009).

[73] A. Kulesza and L. Motyka, Soft gluon resummation for the production of gluino-gluino and squark-antisquark pairs at the LHC, Phys. Rev. D **80**, 095004 (2009).
[74] W. Beenakker, S. Brensing, M. Krämer, A. Kulesza, E. Laenen, and I. Niessen, Soft-gluon resummation for squark and gluino hadroproduction, J. High Energy Phys. 12 (2009) 041.
[75] W. Beenakker, S. Brensing, M. Krämer, A. Kulesza, E. Laenen, L. Motyka, and I. Niessen, Squark and gluino hadroproduction, Int. J. Mod. Phys. A **26**, 2637 (2011).
[76] C. Borschensky, M. Krämer, A. Kulesza, M. Mangano, S. Padhi, T. Plehn, and X. Portell, Squark and gluino production cross sections in pp collisions at $\sqrt{s} = 13$, 14, 33 and 100 TeV, Eur. Phys. J. C **74**, 3174 (2014).
[77] CMS Collaboration, CERN Report No. CMS-PAS-PFT-09-001, 2009, http://cdsweb.cern.ch/record/1194487.
[78] CMS Collaboration, CERN Report No. CMS-PAS-PFT-10-001, 2010, http://cdsweb.cern.ch/record/1247373.
[79] M. Cacciari, G. P. Salam, and G. Soyez, The anti-k_t jet clustering algorithm, J. High Energy Phys. 04 (2008) 063.
[80] M. Cacciari, G. P. Salam, and G. Soyez, FastJet user manual, Eur. Phys. J. C **72**, 1896 (2012).
[81] CMS Collaboration, CERN Report No. CMS-PAS-JME-10-003, 2010, http://cdsweb.cern.ch/record/1279362.
[82] CMS Collaboration, Jet energy scale and resolution in the CMS experiment in pp collisions at 8 TeV, arXiv:1607.03663.
[83] CMS Collaboration, Performance of electron reconstruction and selection with the CMS detector in proton-proton collisions at $\sqrt{s} = 8$ TeV, J. Instrum. **10**, P06005 (2015).
[84] CMS Collaboration , CERN Report No. CMS-PAS-JME-14-001, 2014, http://cds.cern.ch/record/1751454.
[85] CMS Collaboration, Performance of CMS muon reconstruction in pp collision events at $\sqrt{s} = 7$ TeV, J. Instrum. **7**, P10002 (2012).
[86] CMS Collaboration, Reconstruction and identification of τ lepton decays to hadrons and ν_τ at CMS, J. Instrum. **11**, P01019 (2016).
[87] CMS Collaboration, CERN Report No. CMS-PAS-BTV-15-001, 2016, http://cds.cern.ch/record/1751454.
[88] CMS Collaboration, Identification of b-quark jets with the CMS experiment, J. Instrum. **8**, P04013 (2013).
[89] CMS Collaboration, Performance of photon reconstruction and identification with the CMS detector in proton-proton collisions at $\sqrt{s} = 8$ TeV, J. Instrum. **10**, P08010 (2015).
[90] CMS Collaboration, Missing transverse energy performance of the CMS detector, J. Instrum. **6**, P09001 (2011).
[91] CMS Collaboration, Performance of the CMS missing transverse momentum reconstruction in pp data at $\sqrt{s} = 8$ TeV, J. Instrum. **10**, P02006 (2015).
[92] T. Junk, Confidence level computation for combining searches with small statistics, Nucl. Instrum. Methods Phys. Res., Sect. A **434**, 435 (1999).
[93] A. L. Read, Presentation of search results: the CL_s technique, J. Phys. G **28**, 2693 (2002).
[94] A. L. Read, Report No. CERN-OPEN-2000-205, 2000, http://cds.cern.ch/record/451614.
[95] G. Cowan, K. Cranmer, E. Gross, and O. Vitells, Asymptotic formulae for likelihood-based tests of new physics, Eur. Phys. J. C **71**, 1554 (2011).
[96] ATLAS and CMS Collaborations, CERN Technical Reports No. ATL-PHYS-PUB-2011-011 and No. CMS-NOTE-2011-005, 2011.
[97] CMS Collaboration, CERN Technical Report No. CMS-PAS-LUM-15-001, 2016, https://cds.cern.ch/record/2138682.
[98] K. A. Olive *et al.* (Particle Data Group Collaboration), Review of particle physics, Chin. Phys. C **38**, 090001 (2014).
[99] M. Dine, A. Kagan, and S. Samuel, Naturalness in supersymmetry, or raising the supersymmetry breaking scale, Phys. Lett. B **243**, 250 (1990).
[100] A. G. Cohen, D. B. Kaplan, and A. E. Nelson, The more Minimal Supersymmetric Standard Model, Phys. Lett. B **388**, 588 (1996).

V. Khachatryan,[1] A. M. Sirunyan,[1] A. Tumasyan,[1] W. Adam,[2] E. Asilar,[2] T. Bergauer,[2] J. Brandstetter,[2] E. Brondolin,[2] M. Dragicevic,[2] J. Erö,[2] M. Flechl,[2] M. Friedl,[2] R. Frühwirth,[2,b] V. M. Ghete,[2] C. Hartl,[2] N. Hörmann,[2] J. Hrubec,[2] M. Jeitler,[2,b] A. König,[2] I. Krätschmer,[2] D. Liko,[2] T. Matsushita,[2] I. Mikulec,[2] D. Rabady,[2] N. Rad,[2] B. Rahbaran,[2] H. Rohringer,[2] J. Schieck,[2,b] J. Strauss,[2] W. Treberer-Treberspurg,[2] W. Waltenberger,[2] C.-E. Wulz,[2,b] V. Mossolov,[3] N. Shumeiko,[3] J. Suarez Gonzalez,[3] S. Alderweireldt,[4] E. A. De Wolf,[4] X. Janssen,[4] J. Lauwers,[4] M. Van De Klundert,[4] H. Van Haevermaet,[4] P. Van Mechelen,[4] N. Van Remortel,[4] A. Van Spilbeeck,[4] S. Abu Zeid,[5] F. Blekman,[5] J. D'Hondt,[5] N. Daci,[5] I. De Bruyn,[5] K. Deroover,[5] N. Heracleous,[5] S. Lowette,[5] S. Moortgat,[5] L. Moreels,[5] A. Olbrechts,[5] Q. Python,[5] S. Tavernier,[5] W. Van Doninck,[5] P. Van Mulders,[5] I. Van Parijs,[5] H. Brun,[6] C. Caillol,[6] B. Clerbaux,[6] G. De Lentdecker,[6] H. Delannoy,[6] G. Fasanella,[6] L. Favart,[6] R. Goldouzian,[6] A. Grebenyuk,[6] G. Karapostoli,[6] T. Lenzi,[6] A. Léonard,[6] J. Luetic,[6] T. Maerschalk,[6] A. Marinov,[6] A. Randle-conde,[6] T. Seva,[6] C. Vander Velde,[6] P. Vanlaer,[6] R. Yonamine,[6] F. Zenoni,[6] F. Zhang,[6,c] A. Cimmino,[7] T. Cornelis,[7] D. Dobur,[7] A. Fagot,[7] G. Garcia,[7] M. Gul,[7] D. Poyraz,[7] S. Salva,[7] R. Schöfbeck,[7] M. Tytgat,[7] W. Van Driessche,[7] E. Yazgan,[7] N. Zaganidis,[7] H. Bakhshiansohi,[8] C. Beluffi,[8,d] O. Bondu,[8] S. Brochet,[8] G. Bruno,[8] A. Caudron,[8] S. De Visscher,[8] C. Delaere,[8] M. Delcourt,[8] B. Francois,[8] A. Giammanco,[8] A. Jafari,[8] P. Jez,[8] M. Komm,[8] V. Lemaitre,[8] A. Magitteri,[8] A. Mertens,[8] M. Musich,[8] C. Nuttens,[8] K. Piotrzkowski,[8] L. Quertenmont,[8] M. Selvaggi,[8] M. Vidal Marono,[8] S. Wertz,[8] N. Beliy,[9] W. L. Aldá Júnior,[10] F. L. Alves,[10] G. A. Alves,[10] L. Brito,[10]

C. Hensel,[10] A. Moraes,[10] M. E. Pol,[10] P. Rebello Teles,[10] E. Belchior Batista Das Chagas,[11] W. Carvalho,[11] J. Chinellato,[11,e] A. Custódio,[11] E. M. Da Costa,[11] G. G. Da Silveira,[11,f] D. De Jesus Damiao,[11] C. De Oliveira Martins,[11] S. Fonseca De Souza,[11] L. M. Huertas Guativa,[11] H. Malbouisson,[11] D. Matos Figueiredo,[11] C. Mora Herrera,[11] L. Mundim,[11] H. Nogima,[11] W. L. Prado Da Silva,[11] A. Santoro,[11] A. Sznajder,[11] E. J. Tonelli Manganote,[11,e] A. Vilela Pereira,[11] S. Ahuja,[12a] C. A. Bernardes,[12b] S. Dogra,[12a] T. R. Fernandez Perez Tomei,[12a] E. M. Gregores,[12b] P. G. Mercadante,[12b] C. S. Moon,[12a] S. F. Novaes,[12a] Sandra S. Padula,[12a] D. Romero Abad,[12b] J. C. Ruiz Vargas,[12a] A. Aleksandrov,[13] R. Hadjiiska,[13] P. Iaydjiev,[13] M. Rodozov,[13] S. Stoykova,[13] G. Sultanov,[13] M. Vutova,[13] A. Dimitrov,[14] I. Glushkov,[14] L. Litov,[14] B. Pavlov,[14] P. Petkov,[14] W. Fang,[15,g] M. Ahmad,[16] J. G. Bian,[16] G. M. Chen,[16] H. S. Chen,[16] M. Chen,[16] Y. Chen,[16,h] T. Cheng,[16] C. H. Jiang,[16] D. Leggat,[16] Z. Liu,[16] F. Romeo,[16] S. M. Shaheen,[16] A. Spiezia,[16] J. Tao,[16] C. Wang,[16] Z. Wang,[16] H. Zhang,[16] J. Zhao,[16] Y. Ban,[17] G. Chen,[17] Q. Li,[17] S. Liu,[17] Y. Mao,[17] S. J. Qian,[17] D. Wang,[17] Z. Xu,[17] C. Avila,[18] A. Cabrera,[18] L. F. Chaparro Sierra,[18] C. Florez,[18] J. P. Gomez,[18] C. F. González Hernández,[18] J. D. Ruiz Alvarez,[18] J. C. Sanabria,[18] N. Godinovic,[19] D. Lelas,[19] I. Puljak,[19] P. M. Ribeiro Cipriano,[19] T. Sculac,[19] Z. Antunovic,[20] M. Kovac,[20] V. Brigljevic,[21] D. Ferencek,[21] K. Kadija,[21] S. Micanovic,[21] L. Sudic,[21] T. Susa,[21] A. Attikis,[22] G. Mavromanolakis,[22] J. Mousa,[22] C. Nicolaou,[22] F. Ptochos,[22] P. A. Razis,[22] H. Rykaczewski,[22] M. Finger,[23,i] M. Finger Jr.,[23,i] E. Carrera Jarrin,[24] Y. Assran,[25,j,k] T. Elkafrawy,[25,l] A. Mahrous,[25,m] B. Calpas,[26] M. Kadastik,[26] M. Murumaa,[26] L. Perrini,[26] M. Raidal,[26] A. Tiko,[26] C. Veelken,[26] P. Eerola,[27] J. Pekkanen,[27] M. Voutilainen,[27] J. Härkönen,[28] V. Karimäki,[28] R. Kinnunen,[28] T. Lampén,[28] K. Lassila-Perini,[28] S. Lehti,[28] T. Lindén,[28] P. Luukka,[28] T. Peltola,[28] J. Tuominiemi,[28] E. Tuovinen,[28] L. Wendland,[28] J. Talvitie,[29] T. Tuuva,[29] M. Besancon,[30] F. Couderc,[30] M. Dejardin,[30] D. Denegri,[30] B. Fabbro,[30] J. L. Faure,[30] C. Favaro,[30] F. Ferri,[30] S. Ganjour,[30] S. Ghosh,[30] A. Givernaud,[30] P. Gras,[30] G. Hamel de Monchenault,[30] P. Jarry,[30] I. Kucher,[30] E. Locci,[30] M. Machet,[30] J. Malcles,[30] J. Rander,[30] A. Rosowsky,[30] M. Titov,[30] A. Zghiche,[30] A. Abdulsalam,[31] I. Antropov,[31] S. Baffioni,[31] F. Beaudette,[31] P. Busson,[31] L. Cadamuro,[31] E. Chapon,[31] C. Charlot,[31] O. Davignon,[31] R. Granier de Cassagnac,[31] M. Jo,[31] S. Lisniak,[31] P. Miné,[31] M. Nguyen,[31] C. Ochando,[31] G. Ortona,[31] P. Paganini,[31] P. Pigard,[31] S. Regnard,[31] R. Salerno,[31] Y. Sirois,[31] T. Strebler,[31] Y. Yilmaz,[31] A. Zabi,[31] J.-L. Agram,[32,n] J. Andrea,[32] A. Aubin,[32] D. Bloch,[32] J.-M. Brom,[32] M. Buttignol,[32] E. C. Chabert,[32] N. Chanon,[32] C. Collard,[32] E. Conte,[32,n] X. Coubez,[32] J.-C. Fontaine,[32,n] D. Gelé,[32] U. Goerlach,[32] A.-C. Le Bihan,[32] J. A. Merlin,[32,o] K. Skovpen,[32] P. Van Hove,[32] S. Gadrat,[33] S. Beauceron,[34] C. Bernet,[34] G. Boudoul,[34] E. Bouvier,[34] C. A. Carrillo Montoya,[34] R. Chierici,[34] D. Contardo,[34] B. Courbon,[34] P. Depasse,[34] H. El Mamouni,[34] J. Fan,[34] J. Fay,[34] S. Gascon,[34] M. Gouzevitch,[34] G. Grenier,[34] B. Ille,[34] F. Lagarde,[34] I. B. Laktineh,[34] M. Lethuillier,[34] L. Mirabito,[34] A. L. Pequegnot,[34] S. Perries,[34] A. Popov,[34,p] D. Sabes,[34] V. Sordini,[34] M. Vander Donckt,[34] P. Verdier,[34] S. Viret,[34] T. Toriashvili,[35,q] Z. Tsamalaidze,[36,i] C. Autermann,[37] S. Beranek,[37] L. Feld,[37] A. Heister,[37] M. K. Kiesel,[37] K. Klein,[37] M. Lipinski,[37] A. Ostapchuk,[37] M. Preuten,[37] F. Raupach,[37] S. Schael,[37] C. Schomakers,[37] J. F. Schulte,[37] J. Schulz,[37] T. Verlage,[37] H. Weber,[37] V. Zhukov,[37,p] M. Brodski,[38] E. Dietz-Laursonn,[38] D. Duchardt,[38] M. Endres,[38] M. Erdmann,[38] S. Erdweg,[38] T. Esch,[38] R. Fischer,[38] A. Güth,[38] M. Hamer,[38] T. Hebbeker,[38] C. Heidemann,[38] K. Hoepfner,[38] S. Knutzen,[38] M. Merschmeyer,[38] A. Meyer,[38] P. Millet,[38] S. Mukherjee,[38] M. Olschewski,[38] K. Padeken,[38] T. Pook,[38] M. Radziej,[38] H. Reithler,[38] M. Rieger,[38] F. Scheuch,[38] L. Sonnenschein,[38] D. Teyssier,[38] S. Thüer,[38] V. Cherepanov,[39] G. Flügge,[39] W. Haj Ahmad,[39] F. Hoehle,[39] B. Kargoll,[39] T. Kress,[39] A. Künsken,[39] J. Lingemann,[39] T. Müller,[39] A. Nehrkorn,[39] A. Nowack,[39] I. M. Nugent,[39] C. Pistone,[39] O. Pooth,[39] A. Stahl,[39,o] M. Aldaya Martin,[40] C. Asawatangtrakuldee,[40] K. Beernaert,[40] O. Behnke,[40] U. Behrens,[40] A. A. Bin Anuar,[40] K. Borras,[40,r] A. Campbell,[40] P. Connor,[40] C. Contreras-Campana,[40] F. Costanza,[40] C. Diez Pardos,[40] G. Dolinska,[40] G. Eckerlin,[40] D. Eckstein,[40] E. Eren,[40] E. Gallo,[40,s] J. Garay Garcia,[40] A. Geiser,[40] A. Gizhko,[40] J. M. Grados Luyando,[40] P. Gunnellini,[40] A. Harb,[40] J. Hauk,[40] M. Hempel,[40,t] H. Jung,[40] A. Kalogeropoulos,[40] O. Karacheban,[40,t] M. Kasemann,[40] J. Keaveney,[40] J. Kieseler,[40] C. Kleinwort,[40] I. Korol,[40] D. Krücker,[40] W. Lange,[40] A. Lelek,[40] J. Leonard,[40] K. Lipka,[40] A. Lobanov,[40] W. Lohmann,[40,t] R. Mankel,[40] I.-A. Melzer-Pellmann,[40] A. B. Meyer,[40] G. Mittag,[40] J. Mnich,[40] A. Mussgiller,[40] E. Ntomari,[40] D. Pitzl,[40] R. Placakyte,[40] A. Raspereza,[40] B. Roland,[40] M. Ö. Sahin,[40] P. Saxena,[40] T. Schoerner-Sadenius,[40] C. Seitz,[40] S. Spannagel,[40] N. Stefaniuk,[40] K. D. Trippkewitz,[40] G. P. Van Onsem,[40] R. Walsh,[40] C. Wissing,[40] V. Blobel,[41] M. Centis Vignali,[41] A. R. Draeger,[41] T. Dreyer,[41] E. Garutti,[41] D. Gonzalez,[41] J. Haller,[41] M. Hoffmann,[41] A. Junkes,[41] R. Klanner,[41] R. Kogler,[41] N. Kovalchuk,[41] T. Lapsien,[41] T. Lenz,[41] I. Marchesini,[41] D. Marconi,[41] M. Meyer,[41] M. Niedziela,[41] D. Nowatschin,[41] F. Pantaleo,[41,o] T. Peiffer,[41] A. Perieanu,[41] J. Poehlsen,[41] C. Sander,[41] C. Scharf,[41] P. Schleper,[41] A. Schmidt,[41] S. Schumann,[41] J. Schwandt,[41] H. Stadie,[41] G. Steinbrück,[41] F. M. Stober,[41] M. Stöver,[41]

H. Tholen,[41] D. Troendle,[41] E. Usai,[41] L. Vanelderen,[41] A. Vanhoefer,[41] B. Vormwald,[41] C. Barth,[42] C. Baus,[42] J. Berger,[42] E. Butz,[42] T. Chwalek,[42] F. Colombo,[42] W. De Boer,[42] A. Dierlamm,[42] S. Fink,[42] R. Friese,[42] M. Giffels,[42] A. Gilbert,[42] P. Goldenzweig,[42] D. Haitz,[42] F. Hartmann,[42,o] S. M. Heindl,[42] U. Husemann,[42] I. Katkov,[42,p] P. Lobelle Pardo,[42] B. Maier,[42] H. Mildner,[42] M. U. Mozer,[42] Th. Müller,[42] M. Plagge,[42] G. Quast,[42] K. Rabbertz,[42] S. Röcker,[42] F. Roscher,[42] M. Schröder,[42] I. Shvetsov,[42] G. Sieber,[42] H. J. Simonis,[42] R. Ulrich,[42] J. Wagner-Kuhr,[42] S. Wayand,[42] M. Weber,[42] T. Weiler,[42] S. Williamson,[42] C. Wöhrmann,[42] R. Wolf,[42] G. Anagnostou,[43] G. Daskalakis,[43] T. Geralis,[43] V. A. Giakoumopoulou,[43] A. Kyriakis,[43] D. Loukas,[43] I. Topsis-Giotis,[43] A. Agapitos,[44] S. Kesisoglou,[44] A. Panagiotou,[44] N. Saoulidou,[44] E. Tziaferi,[44] I. Evangelou,[45] G. Flouris,[45] C. Foudas,[45] P. Kokkas,[45] N. Loukas,[45] N. Manthos,[45] I. Papadopoulos,[45] E. Paradas,[45] N. Filipovic,[46] G. Bencze,[47] C. Hajdu,[47] P. Hidas,[47] D. Horvath,[47,u] F. Sikler,[47] V. Veszpremi,[47] G. Vesztergombi,[47,v] A. J. Zsigmond,[47] N. Beni,[48] S. Czellar,[48] J. Karancsi,[48,w] A. Makovec,[48] J. Molnar,[48] Z. Szillasi,[48] M. Bartók,[49,v] P. Raics,[49] Z. L. Trocsanyi,[49] B. Ujvari,[49] S. Bahinipati,[50] S. Choudhury,[50,x] P. Mal,[50] K. Mandal,[50] A. Nayak,[50,y] D. K. Sahoo,[50] N. Sahoo,[50] S. K. Swain,[50] S. Bansal,[51] S. B. Beri,[51] V. Bhatnagar,[51] R. Chawla,[51] U. Bhawandeep,[51] A. K. Kalsi,[51] A. Kaur,[51] M. Kaur,[51] R. Kumar,[51] A. Mehta,[51] M. Mittal,[51] J. B. Singh,[51] G. Walia,[51] Ashok Kumar,[52] A. Bhardwaj,[52] B. C. Choudhary,[52] R. B. Garg,[52] S. Keshri,[52] S. Malhotra,[52] M. Naimuddin,[52] N. Nishu,[52] K. Ranjan,[52] R. Sharma,[52] V. Sharma,[52] R. Bhattacharya,[53] S. Bhattacharya,[53] K. Chatterjee,[53] S. Dey,[53] S. Dutt,[53] S. Dutta,[53] S. Ghosh,[53] N. Majumdar,[53] A. Modak,[53] K. Mondal,[53] S. Mukhopadhyay,[53] S. Nandan,[53] A. Purohit,[53] A. Roy,[53] D. Roy,[53] S. Roy Chowdhury,[53] S. Sarkar,[53] M. Sharan,[53] S. Thakur,[53] P. K. Behera,[54] R. Chudasama,[55] D. Dutta,[55] V. Jha,[55] V. Kumar,[55] A. K. Mohanty,[55,o] P. K. Netrakanti,[55] L. M. Pant,[55] P. Shukla,[55] A. Topkar,[55] T. Aziz,[56] S. Dugad,[56] G. Kole,[56] B. Mahakud,[56] S. Mitra,[56] G. B. Mohanty,[56] B. Parida,[56] N. Sur,[56] B. Sutar,[56] S. Banerjee,[57] S. Bhowmik,[57,z] R. K. Dewanjee,[57] S. Ganguly,[57] M. Guchait,[57] Sa. Jain,[57] S. Kumar,[57] M. Maity,[57,z] G. Majumder,[57] K. Mazumdar,[57] T. Sarkar,[57,z] N. Wickramage,[57,aa] S. Chauhan,[58] S. Dube,[58] V. Hegde,[58] A. Kapoor,[58] K. Kothekar,[58] A. Rane,[58] S. Sharma,[58] H. Behnamian,[59] S. Chenarani,[59,bb] E. Eskandari Tadavani,[59] S. M. Etesami,[59,bb] A. Fahim,[59,cc] M. Khakzad,[59] M. Mohammadi Najafabadi,[59] M. Naseri,[59] S. Paktinat Mehdiabadi,[59,dd] F. Rezaei Hosseinabadi,[59] B. Safarzadeh,[59,ee] M. Zeinali,[59] M. Felcini,[60] M. Grunewald,[60] M. Abbrescia,[61a,61b] C. Calabria,[61a,61b] C. Caputo,[61a,61b] A. Colaleo,[61a] D. Creanza,[61a,61c] L. Cristella,[61a,61b] N. De Filippis,[61a,61c] M. De Palma,[61a,61b] L. Fiore,[61a] G. Iaselli,[61a,61c] G. Maggi,[61a,61c] M. Maggi,[61a] G. Miniello,[61a,61b] S. My,[61a,61b] S. Nuzzo,[61a,61b] A. Pompili,[61a,61b] G. Pugliese,[61a,61c] R. Radogna,[61a,61b] A. Ranieri,[61a] G. Selvaggi,[61a,61b] L. Silvestris,[61a,o] R. Venditti,[61a,61b] P. Verwilligen,[61a] G. Abbiendi,[62a] C. Battilana,[62a] D. Bonacorsi,[62a,62b] S. Braibant-Giacomelli,[62a,62b] L. Brigliadori,[62a,62b] R. Campanini,[62a,62b] P. Capiluppi,[62a,62b] A. Castro,[62a,62b] F. R. Cavallo,[62a] S. S. Chhibra,[62a,62b] G. Codispoti,[62a,62b] M. Cuffiani,[62a,62b] G. M. Dallavalle,[62a] F. Fabbri,[62a] A. Fanfani,[62a,62b] D. Fasanella,[62a,62b] P. Giacomelli,[62a] C. Grandi,[62a] L. Guiducci,[62a,62b] S. Marcellini,[62a] G. Masetti,[62a] A. Montanari,[62a] F. L. Navarria,[62a,62b] A. Perrotta,[62a] A. M. Rossi,[62a,62b] T. Rovelli,[62a,62b] G. P. Siroli,[62a,62b] N. Tosi,[62a,62b,o] S. Albergo,[63a,63b] M. Chiorboli,[63a,63b] S. Costa,[63a,63b] A. Di Mattia,[63a] F. Giordano,[63a,63b] R. Potenza,[63a,63b] A. Tricomi,[63a,63b] C. Tuve,[63a,63b] G. Barbagli,[64a] V. Ciulli,[64a,64b] C. Civinini,[64a] R. D'Alessandro,[64a,64b] E. Focardi,[64a,64b] V. Gori,[64a,64b] P. Lenzi,[64a,64b] M. Meschini,[64a] S. Paoletti,[64a] G. Sguazzoni,[64a] L. Viliani,[64a,64b,o] L. Benussi,[65] S. Bianco,[65] F. Fabbri,[65] D. Piccolo,[65] F. Primavera,[65,o] V. Calvelli,[66a,66b] F. Ferro,[66a] M. Lo Vetere,[66a,66b] M. R. Monge,[66a,66b] E. Robutti,[66a] S. Tosi,[66a,66b] L. Brianza,[67a,o] M. E. Dinardo,[67a,67b] S. Fiorendi,[67a,67b] S. Gennai,[67a] A. Ghezzi,[67a,67b] P. Govoni,[67a,67b] M. Malberti,[67a] S. Malvezzi,[67a] R. A. Manzoni,[67a,67b,o] B. Marzocchi,[67a,67b] D. Menasce,[67a] L. Moroni,[67a] M. Paganoni,[67a,67b] D. Pedrini,[67a] S. Pigazzini,[67a] S. Ragazzi,[67a,67b] T. Tabarelli de Fatis,[67a,67b] S. Buontempo,[68a] N. Cavallo,[68a,68c] G. De Nardo,[68a] S. Di Guida,[68a,68d,o] M. Esposito,[68a,68b] F. Fabozzi,[68a,68c] A. O. M. Iorio,[68a,68b] G. Lanza,[68a] L. Lista,[68a] S. Meola,[68a,68d,o] P. Paolucci,[68a,o] C. Sciacca,[68a,68b] F. Thyssen,[68a] P. Azzi,[69a,o] N. Bacchetta,[69a] L. Benato,[69a,69b] D. Bisello,[69a,69b] A. Boletti,[69a,69b] R. Carlin,[69a,69b] A. Carvalho Antunes De Oliveira,[69a,69b] P. Checchia,[69a] M. Dall'Osso,[69a,69b] P. De Castro Manzano,[69a] T. Dorigo,[69a] U. Dosselli,[69a] F. Gasparini,[69a,69b] U. Gasparini,[69a,69b] A. Gozzelino,[69a] S. Lacaprara,[69a] M. Margoni,[69a,69b] A. T. Meneguzzo,[69a,69b] J. Pazzini,[69a,69b,o] N. Pozzobon,[69a,69b] P. Ronchese,[69a,69b] F. Simonetto,[69a,69b] E. Torassa,[69a] M. Zanetti,[69a] P. Zotto,[69a,69b] A. Zucchetta,[69a,69b] G. Zumerle,[69a,69b] A. Braghieri,[70a] A. Magnani,[70a,70b] P. Montagna,[70a,70b] S. P. Ratti,[70a,70b] V. Re,[70a] C. Riccardi,[70a,70b] P. Salvini,[70a] I. Vai,[70a,70b] P. Vitulo,[70a,70b] L. Alunni Solestizi,[71a,71b] G. M. Bilei,[71a] D. Ciangottini,[71a,71b] L. Fanò,[71a,71b] P. Lariccia,[71a,71b] R. Leonardi,[71a,71b] G. Mantovani,[71a,71b] M. Menichelli,[71a] A. Saha,[71a] A. Santocchia,[71a,71b] K. Androsov,[72a,ff] P. Azzurri,[72a,o] G. Bagliesi,[72a] J. Bernardini,[72a] T. Boccali,[72a] R. Castaldi,[72a] M. A. Ciocci,[72a,ff] R. Dell'Orso,[72a] S. Donato,[72a,72c] G. Fedi,[72a] A. Giassi,[72a] M. T. Grippo,[72a,ff] F. Ligabue,[72a,72c] T. Lomtadze,[72a] L. Martini,[72a,72b] A. Messineo,[72a,72b] F. Palla,[72a]

A. Rizzi,[72a,72b] A. Savoy-Navarro,[72a,gg] P. Spagnolo,[72a] R. Tenchini,[72a] G. Tonelli,[72a,72b] A. Venturi,[72a] P. G. Verdini,[72a] L. Barone,[73a,73b] F. Cavallari,[73a] M. Cipriani,[73a,73b] G. D'imperio,[73a,73b,o] D. Del Re,[73a,73b,o] M. Diemoz,[73a] S. Gelli,[73a,73b] E. Longo,[73a,73b] F. Margaroli,[73a,73b] P. Meridiani,[73a] G. Organtini,[73a,73b] R. Paramatti,[73a] F. Preiato,[73a,73b] S. Rahatlou,[73a,73b] C. Rovelli,[73a] F. Santanastasio,[73a,73b] N. Amapane,[74a,74b] R. Arcidiacono,[74a,74c,o] S. Argiro,[74a,74b] M. Arneodo,[74a,74c] N. Bartosik,[74a] R. Bellan,[74a,74b] C. Biino,[74a] N. Cartiglia,[74a] F. Cenna,[74a,74b] M. Costa,[74a,74b] R. Covarelli,[74a,74b] A. Degano,[74a,74b] N. Demaria,[74a] L. Finco,[74a,74b] B. Kiani,[74a,74b] C. Mariotti,[74a] S. Maselli,[74a] E. Migliore,[74a,74b] V. Monaco,[74a,74b] E. Monteil,[74a,74b] M. M. Obertino,[74a,74b] L. Pacher,[74a,74b] N. Pastrone,[74a] M. Pelliccioni,[74a] G. L. Pinna Angioni,[74a,74b] F. Ravera,[74a,74b] A. Romero,[74a,74b] M. Ruspa,[74a,74c] R. Sacchi,[74a,74b] K. Shchelina,[74a,74b] V. Sola,[74a] A. Solano,[74a,74b] A. Staiano,[74a] P. Traczyk,[74a,74b] S. Belforte,[75a] M. Casarsa,[75a] F. Cossutti,[75a] G. Della Ricca,[75a,75b] C. La Licata,[75a,75b] A. Schizzi,[75a,75b] A. Zanetti,[75a] D. H. Kim,[76] G. N. Kim,[76] M. S. Kim,[76] S. Lee,[76] S. W. Lee,[76] Y. D. Oh,[76] S. Sekmen,[76] D. C. Son,[76] Y. C. Yang,[76] A. Lee,[77] J. A. Brochero Cifuentes,[78] T. J. Kim,[78] S. Cho,[79] S. Choi,[79] Y. Go,[79] D. Gyun,[79] S. Ha,[79] B. Hong,[79] Y. Jo,[79] Y. Kim,[79] B. Lee,[79] K. Lee,[79] K. S. Lee,[79] S. Lee,[79] J. Lim,[79] S. K. Park,[79] Y. Roh,[79] J. Almond,[80] J. Kim,[80] H. Lee,[80] S. B. Oh,[80] B. C. Radburn-Smith,[80] S. h. Seo,[80] U. K. Yang,[80] H. D. Yoo,[80] G. B. Yu,[80] M. Choi,[81] H. Kim,[81] H. Kim,[81] J. H. Kim,[81] J. S. H. Lee,[81] I. C. Park,[81] G. Ryu,[81] M. S. Ryu,[81] Y. Choi,[82] J. Goh,[82] C. Hwang,[82] J. Lee,[82] I. Yu,[82] V. Dudenas,[83] A. Juodagalvis,[83] J. Vaitkus,[83] I. Ahmed,[84] Z. A. Ibrahim,[84] J. R. Komaragiri,[84] M. A. B. Md Ali,[84,hh] F. Mohamad Idris,[84,ii] W. A. T. Wan Abdullah,[84] M. N. Yusli,[84] Z. Zolkapli,[84] H. Castilla-Valdez,[85] E. De La Cruz-Burelo,[85] I. Heredia-De La Cruz,[85,jj] A. Hernandez-Almada,[85] R. Lopez-Fernandez,[85] R. Magaña Villalba,[85] J. Mejia Guisao,[85] A. Sanchez-Hernandez,[85] S. Carrillo Moreno,[86] C. Oropeza Barrera,[86] F. Vazquez Valencia,[86] S. Carpinteyro,[87] I. Pedraza,[87] H. A. Salazar Ibarguen,[87] C. Uribe Estrada,[87] A. Morelos Pineda,[88] D. Krofcheck,[89] P. H. Butler,[90] A. Ahmad,[91] M. Ahmad,[91] Q. Hassan,[91] H. R. Hoorani,[91] W. A. Khan,[91] M. A. Shah,[91] M. Shoaib,[91] M. Waqas,[91] H. Bialkowska,[92] M. Bluj,[92] B. Boimska,[92] T. Frueboes,[92] M. Górski,[92] M. Kazana,[92] K. Nawrocki,[92] K. Romanowska-Rybinska,[92] M. Szleper,[92] P. Zalewski,[92] K. Bunkowski,[93] A. Byszuk,[93,kk] K. Doroba,[93] A. Kalinowski,[93] M. Konecki,[93] J. Krolikowski,[93] M. Misiura,[93] M. Olszewski,[93] M. Walczak,[93] P. Bargassa,[94] C. Beirão Da Cruz E Silva,[94] A. Di Francesco,[94] P. Faccioli,[94] P. G. Ferreira Parracho,[94] M. Gallinaro,[94] J. Hollar,[94] N. Leonardo,[94] L. Lloret Iglesias,[94] M. V. Nemallapudi,[94] J. Rodrigues Antunes,[94] J. Seixas,[94] O. Toldaiev,[94] D. Vadruccio,[94] J. Varela,[94] P. Vischia,[94] S. Afanasiev,[95] V. Alexakhin,[95] M. Gavrilenko,[95] I. Golutvin,[95] I. Gorbunov,[95] A. Kamenev,[95] V. Karjavin,[95] A. Lanev,[95] A. Malakhov,[95] V. Matveev,[95,ll,mm] P. Moisenz,[95] V. Palichik,[95] V. Perelygin,[95] M. Savina,[95] S. Shmatov,[95] N. Skatchkov,[95] V. Smirnov,[95] N. Voytishin,[95] A. Zarubin,[95] L. Chtchipounov,[96] V. Golovtsov,[96] Y. Ivanov,[96] V. Kim,[96,nn] E. Kuznetsova,[96,oo] V. Murzin,[96] V. Oreshkin,[96] V. Sulimov,[96] A. Vorobyev,[96] Yu. Andreev,[97] A. Dermenev,[97] S. Gninenko,[97] N. Golubev,[97] A. Karneyeu,[97] M. Kirsanov,[97] N. Krasnikov,[97] A. Pashenkov,[97] D. Tlisov,[97] A. Toropin,[97] V. Epshteyn,[98] V. Gavrilov,[98] N. Lychkovskaya,[98] V. Popov,[98] I. Pozdnyakov,[98] G. Safronov,[98] A. Spiridonov,[98] M. Toms,[98] E. Vlasov,[98] A. Zhokin,[98] A. Bylinkin,[99,mm] R. Chistov,[100,pp] M. Danilov,[100,pp] V. Rusinov,[100] V. Andreev,[101] M. Azarkin,[101,mm] I. Dremin,[101,mm] M. Kirakosyan,[101] A. Leonidov,[101,mm] S. V. Rusakov,[101] A. Terkulov,[101] A. Baskakov,[102] A. Belyaev,[102] E. Boos,[102] M. Dubinin,[102,qq] L. Dudko,[102] A. Ershov,[102] A. Gribushin,[102] V. Klyukhin,[102] O. Kodolova,[102] I. Lokhtin,[102] I. Miagkov,[102] S. Obraztsov,[102] S. Petrushanko,[102] V. Savrin,[102] A. Snigirev,[102] V. Blinov,[103,rr] Y. Skovpen,[103,rr] I. Azhgirey,[104] I. Bayshev,[104] S. Bitioukov,[104] D. Elumakhov,[104] V. Kachanov,[104] A. Kalinin,[104] D. Konstantinov,[104] V. Krychkine,[104] V. Petrov,[104] R. Ryutin,[104] A. Sobol,[104] S. Troshin,[104] N. Tyurin,[104] A. Uzunian,[104] A. Volkov,[104] P. Adzic,[105,ss] P. Cirkovic,[105] D. Devetak,[105] M. Dordevic,[105] J. Milosevic,[105] V. Rekovic,[105] J. Alcaraz Maestre,[106] M. Barrio Luna,[106] E. Calvo,[106] M. Cerrada,[106] M. Chamizo Llatas,[106] N. Colino,[106] B. De La Cruz,[106] A. Delgado Peris,[106] A. Escalante Del Valle,[106] C. Fernandez Bedoya,[106] J. P. Fernández Ramos,[106] J. Flix,[106] M. C. Fouz,[106] P. Garcia-Abia,[106] O. Gonzalez Lopez,[106] S. Goy Lopez,[106] J. M. Hernandez,[106] M. I. Josa,[106] E. Navarro De Martino,[106] A. Pérez-Calero Yzquierdo,[106] J. Puerta Pelayo,[106] A. Quintario Olmeda,[106] I. Redondo,[106] L. Romero,[106] M. S. Soares,[106] J. F. de Trocóniz,[107] M. Missiroli,[107] D. Moran,[107] J. Cuevas,[108] J. Fernandez Menendez,[108] I. Gonzalez Caballero,[108] J. R. González Fernández,[108] E. Palencia Cortezon,[108] S. Sanchez Cruz,[108] I. Suárez Andrés,[108] J. M. Vizan Garcia,[108] I. J. Cabrillo,[109] A. Calderon,[109] J. R. Castiñeiras De Saa,[109] E. Curras,[109] M. Fernandez,[109] J. Garcia-Ferrero,[109] G. Gomez,[109] A. Lopez Virto,[109] J. Marco,[109] C. Martinez Rivero,[109] F. Matorras,[109] J. Piedra Gomez,[109] T. Rodrigo,[109] A. Ruiz-Jimeno,[109] L. Scodellaro,[109] N. Trevisani,[109] I. Vila,[109] R. Vilar Cortabitarte,[109] D. Abbaneo,[110] E. Auffray,[110] G. Auzinger,[110] M. Bachtis,[110] P. Baillon,[110] A. H. Ball,[110] D. Barney,[110] P. Bloch,[110] A. Bocci,[110] A. Bonato,[110] C. Botta,[110] T. Camporesi,[110] R. Castello,[110] M. Cepeda,[110] G. Cerminara,[110] M. D'Alfonso,[110] D. d'Enterria,[110] A. Dabrowski,[110]

V. Daponte,[110] A. David,[110] M. De Gruttola,[110] F. De Guio,[110] A. De Roeck,[110] E. Di Marco,[110,tt] M. Dobson,[110] B. Dorney,[110] T. du Pree,[110] D. Duggan,[110] M. Dünser,[110] N. Dupont,[110] A. Elliott-Peisert,[110] S. Fartoukh,[110] G. Franzoni,[110] J. Fulcher,[110] W. Funk,[110] D. Gigi,[110] K. Gill,[110] M. Girone,[110] F. Glege,[110] D. Gulhan,[110] S. Gundacker,[110] M. Guthoff,[110] J. Hammer,[110] P. Harris,[110] J. Hegeman,[110] V. Innocente,[110] P. Janot,[110] H. Kirschenmann,[110] V. Knünz,[110] A. Kornmayer,[110,o] M. J. Kortelainen,[110] K. Kousouris,[110] M. Krammer,[110,b] P. Lecoq,[110] C. Lourenço,[110] M. T. Lucchini,[110] L. Malgeri,[110] M. Mannelli,[110] A. Martelli,[110] F. Meijers,[110] S. Mersi,[110] E. Meschi,[110] F. Moortgat,[110] S. Morovic,[110] M. Mulders,[110] H. Neugebauer,[110] S. Orfanelli,[110] L. Orsini,[110] L. Pape,[110] E. Perez,[110] M. Peruzzi,[110] A. Petrilli,[110] G. Petrucciani,[110] A. Pfeiffer,[110] M. Pierini,[110] A. Racz,[110] T. Reis,[110] G. Rolandi,[110,uu] M. Rovere,[110] M. Ruan,[110] H. Sakulin,[110] J. B. Sauvan,[110] C. Schäfer,[110] C. Schwick,[110] M. Seidel,[110] A. Sharma,[110] P. Silva,[110] M. Simon,[110] P. Sphicas,[110,vv] J. Steggemann,[110] M. Stoye,[110] Y. Takahashi,[110] M. Tosi,[110] D. Treille,[110] A. Triossi,[110] A. Tsirou,[110] V. Veckalns,[110,ww] G. I. Veres,[110,v] N. Wardle,[110] H. K. Wöhri,[110] A. Zagozdzinska,[110,kk] W. D. Zeuner,[110] W. Bertl,[111] K. Deiters,[111] W. Erdmann,[111] R. Horisberger,[111] Q. Ingram,[111] H. C. Kaestli,[111] D. Kotlinski,[111] U. Langenegger,[111] T. Rohe,[111] F. Bachmair,[112] L. Bäni,[112] L. Bianchini,[112] B. Casal,[112] G. Dissertori,[112] M. Dittmar,[112] M. Donegà,[112] P. Eller,[112] C. Grab,[112] C. Heidegger,[112] D. Hits,[112] J. Hoss,[112] G. Kasieczka,[112] P. Lecomte,[112,a] W. Lustermann,[112] B. Mangano,[112] M. Marionneau,[112] P. Martinez Ruiz del Arbol,[112] M. Masciovecchio,[112] M. T. Meinhard,[112] D. Meister,[112] F. Micheli,[112] P. Musella,[112] F. Nessi-Tedaldi,[112] F. Pandolfi,[112] J. Pata,[112] F. Pauss,[112] G. Perrin,[112] L. Perrozzi,[112] M. Quittnat,[112] M. Rossini,[112] M. Schönenberger,[112] A. Starodumov,[112,xx] V. R. Tavolaro,[112] K. Theofilatos,[112] R. Wallny,[112] T. K. Aarrestad,[113] C. Amsler,[113,yy] L. Caminada,[113] M. F. Canelli,[113] A. De Cosa,[113] C. Galloni,[113] A. Hinzmann,[113] T. Hreus,[113] B. Kilminster,[113] C. Lange,[113] J. Ngadiuba,[113] D. Pinna,[113] G. Rauco,[113] P. Robmann,[113] D. Salerno,[113] Y. Yang,[113] V. Candelise,[114] T. H. Doan,[114] Sh. Jain,[114] R. Khurana,[114] M. Konyushikhin,[114] C. M. Kuo,[114] W. Lin,[114] Y. J. Lu,[114] A. Pozdnyakov,[114] S. S. Yu,[114] Arun Kumar,[115] P. Chang,[115] Y. H. Chang,[115] Y. W. Chang,[115] Y. Chao,[115] K. F. Chen,[115] P. H. Chen,[115] C. Dietz,[115] F. Fiori,[115] W.-S. Hou,[115] Y. Hsiung,[115] Y. F. Liu,[115] R.-S. Lu,[115] M. Miñano Moya,[115] E. Paganis,[115] A. Psallidas,[115] J. f. Tsai,[115] Y. M. Tzeng,[115] B. Asavapibhop,[116] G. Singh,[116] N. Srimanobhas,[116] N. Suwonjandee,[116] A. Adiguzel,[117] M. N. Bakirci,[117,zz] S. Cerci,[117,aaa] S. Damarseckin,[117] Z. S. Demiroglu,[117] C. Dozen,[117] I. Dumanoglu,[117] S. Girgis,[117] G. Gokbulut,[117] Y. Guler,[117] E. Gurpinar,[117] I. Hos,[117] E. E. Kangal,[117,bbb] O. Kara,[117] A. Kayis Topaksu,[117] U. Kiminsu,[117] M. Oglakci,[117] G. Onengut,[117,ccc] K. Ozdemir,[117,ddd] B. Tali,[117,aaa] S. Turkcapar,[117] I. S. Zorbakir,[117] C. Zorbilmez,[117] B. Bilin,[118] S. Bilmis,[118] B. Isildak,[118,eee] G. Karapinar,[118,fff] M. Yalvac,[118] M. Zeyrek,[118] E. Gülmez,[119] M. Kaya,[119,ggg] O. Kaya,[119,hhh] E. A. Yetkin,[119,iii] T. Yetkin,[119,jjj] A. Cakir,[120] K. Cankocak,[120] S. Sen,[120,kkk] B. Grynyov,[121] L. Levchuk,[122] P. Sorokin,[122] R. Aggleton,[123] F. Ball,[123] L. Beck,[123] J. J. Brooke,[123] D. Burns,[123] E. Clement,[123] D. Cussans,[123] H. Flacher,[123] J. Goldstein,[123] M. Grimes,[123] G. P. Heath,[123] H. F. Heath,[123] J. Jacob,[123] L. Kreczko,[123] C. Lucas,[123] D. M. Newbold,[123,lll] S. Paramesvaran,[123] A. Poll,[123] T. Sakuma,[123] S. Seif El Nasr-storey,[123] D. Smith,[123] V. J. Smith,[123] K. W. Bell,[124] A. Belyaev,[124,mmm] C. Brew,[124] R. M. Brown,[124] L. Calligaris,[124] D. Cieri,[124] D. J. A. Cockerill,[124] J. A. Coughlan,[124] K. Harder,[124] S. Harper,[124] E. Olaiya,[124] D. Petyt,[124] C. H. Shepherd-Themistocleous,[124] A. Thea,[124] I. R. Tomalin,[124] T. Williams,[124] M. Baber,[125] R. Bainbridge,[125] O. Buchmuller,[125] A. Bundock,[125] D. Burton,[125] S. Casasso,[125] M. Citron,[125] D. Colling,[125] L. Corpe,[125] P. Dauncey,[125] G. Davies,[125] A. De Wit,[125] M. Della Negra,[125] R. Di Maria,[125] P. Dunne,[125] A. Elwood,[125] D. Futyan,[125] Y. Haddad,[125] G. Hall,[125] G. Iles,[125] T. James,[125] R. Lane,[125] C. Laner,[125] R. Lucas,[125,lll] L. Lyons,[125] A.-M. Magnan,[125] S. Malik,[125] L. Mastrolorenzo,[125] J. Nash,[125] A. Nikitenko,[125,xx] J. Pela,[125] B. Penning,[125] M. Pesaresi,[125] D. M. Raymond,[125] A. Richards,[125] A. Rose,[125] C. Seez,[125] S. Summers,[125] A. Tapper,[125] K. Uchida,[125] M. Vazquez Acosta,[125,nnn] T. Virdee,[125,o] J. Wright,[125] S. C. Zenz,[125] J. E. Cole,[126] P. R. Hobson,[126] A. Khan,[126] P. Kyberd,[126] D. Leslie,[126] I. D. Reid,[126] P. Symonds,[126] L. Teodorescu,[126] M. Turner,[126] A. Borzou,[127] K. Call,[127] J. Dittmann,[127] K. Hatakeyama,[127] H. Liu,[127] N. Pastika,[127] O. Charaf,[128] S. I. Cooper,[128] C. Henderson,[128] P. Rumerio,[128] C. West,[128] D. Arcaro,[129] A. Avetisyan,[129] T. Bose,[129] D. Gastler,[129] D. Rankin,[129] C. Richardson,[129] J. Rohlf,[129] L. Sulak,[129] D. Zou,[129] G. Benelli,[130] E. Berry,[130] D. Cutts,[130] A. Garabedian,[130] J. Hakala,[130] U. Heintz,[130] J. M. Hogan,[130] O. Jesus,[130] E. Laird,[130] G. Landsberg,[130] Z. Mao,[130] M. Narain,[130] S. Piperov,[130] S. Sagir,[130] E. Spencer,[130] R. Syarif,[130] R. Breedon,[131] G. Breto,[131] D. Burns,[131] M. Calderon De La Barca Sanchez,[131] S. Chauhan,[131] M. Chertok,[131] J. Conway,[131] R. Conway,[131] P. T. Cox,[131] R. Erbacher,[131] C. Flores,[131] G. Funk,[131] M. Gardner,[131] W. Ko,[131] R. Lander,[131] C. Mclean,[131] M. Mulhearn,[131] D. Pellett,[131] J. Pilot,[131] F. Ricci-Tam,[131] S. Shalhout,[131] J. Smith,[131] M. Squires,[131] D. Stolp,[131] M. Tripathi,[131] S. Wilbur,[131] R. Yohay,[131] R. Cousins,[132] P. Everaerts,[132] A. Florent,[132] J. Hauser,[132] M. Ignatenko,[132] D. Saltzberg,[132] E. Takasugi,[132] V. Valuev,[132]

M. Weber,[132] K. Burt,[133] R. Clare,[133] J. Ellison,[133] J. W. Gary,[133] G. Hanson,[133] J. Heilman,[133] P. Jandir,[133] E. Kennedy,[133] F. Lacroix,[133] O. R. Long,[133] M. Olmedo Negrete,[133] M. I. Paneva,[133] A. Shrinivas,[133] H. Wei,[133] S. Wimpenny,[133] B. R. Yates,[133] J. G. Branson,[134] G. B. Cerati,[134] S. Cittolin,[134] M. Derdzinski,[134] R. Gerosa,[134] A. Holzner,[134] D. Klein,[134] V. Krutelyov,[134] J. Letts,[134] I. Macneill,[134] D. Olivito,[134] S. Padhi,[134] M. Pieri,[134] M. Sani,[134] V. Sharma,[134] S. Simon,[134] M. Tadel,[134] A. Vartak,[134] S. Wasserbaech,[134,ooo] C. Welke,[134] J. Wood,[134] F. Würthwein,[134] A. Yagil,[134] G. Zevi Della Porta,[134] R. Bhandari,[135] J. Bradmiller-Feld,[135] C. Campagnari,[135] A. Dishaw,[135] V. Dutta,[135] K. Flowers,[135] M. Franco Sevilla,[135] P. Geffert,[135] C. George,[135] F. Golf,[135] L. Gouskos,[135] J. Gran,[135] R. Heller,[135] J. Incandela,[135] N. Mccoll,[135] S. D. Mullin,[135] A. Ovcharova,[135] J. Richman,[135] D. Stuart,[135] I. Suarez,[135] J. Yoo,[135] D. Anderson,[136] A. Apresyan,[136] J. Bendavid,[136] A. Bornheim,[136] J. Bunn,[136] Y. Chen,[136] J. Duarte,[136] J. M. Lawhorn,[136] A. Mott,[136] H. B. Newman,[136] C. Pena,[136] M. Spiropulu,[136] J. R. Vlimant,[136] S. Xie,[136] R. Y. Zhu,[136] M. B. Andrews,[137] V. Azzolini,[137] T. Ferguson,[137] M. Paulini,[137] J. Russ,[137] M. Sun,[137] H. Vogel,[137] I. Vorobiev,[137] J. P. Cumalat,[138] W. T. Ford,[138] F. Jensen,[138] A. Johnson,[138] M. Krohn,[138] T. Mulholland,[138] K. Stenson,[138] S. R. Wagner,[138] J. Alexander,[139] J. Chaves,[139] J. Chu,[139] S. Dittmer,[139] K. Mcdermott,[139] N. Mirman,[139] G. Nicolas Kaufman,[139] J. R. Patterson,[139] A. Rinkevicius,[139] A. Ryd,[139] L. Skinnari,[139] L. Soffi,[139] S. M. Tan,[139] Z. Tao,[139] J. Thom,[139] J. Tucker,[139] P. Wittich,[139] M. Zientek,[139] D. Winn,[140] S. Abdullin,[141] M. Albrow,[141] G. Apollinari,[141] S. Banerjee,[141] L. A. T. Bauerdick,[141] A. Beretvas,[141] J. Berryhill,[141] P. C. Bhat,[141] G. Bolla,[141] K. Burkett,[141] J. N. Butler,[141] H. W. K. Cheung,[141] F. Chlebana,[141] S. Cihangir,[141,a] M. Cremonesi,[141] V. D. Elvira,[141] I. Fisk,[141] J. Freeman,[141] E. Gottschalk,[141] L. Gray,[141] D. Green,[141] S. Grünendahl,[141] O. Gutsche,[141] D. Hare,[141] R. M. Harris,[141] S. Hasegawa,[141] J. Hirschauer,[141] Z. Hu,[141] B. Jayatilaka,[141] S. Jindariani,[141] M. Johnson,[141] U. Joshi,[141] B. Klima,[141] B. Kreis,[141] S. Lammel,[141] J. Linacre,[141] D. Lincoln,[141] R. Lipton,[141] T. Liu,[141] R. Lopes De Sá,[141] J. Lykken,[141] K. Maeshima,[141] N. Magini,[141] J. M. Marraffino,[141] S. Maruyama,[141] D. Mason,[141] P. McBride,[141] P. Merkel,[141] S. Mrenna,[141] S. Nahn,[141] C. Newman-Holmes,[141,a] V. O'Dell,[141] K. Pedro,[141] O. Prokofyev,[141] G. Rakness,[141] L. Ristori,[141] E. Sexton-Kennedy,[141] A. Soha,[141] W. J. Spalding,[141] L. Spiegel,[141] S. Stoynev,[141] N. Strobbe,[141] L. Taylor,[141] S. Tkaczyk,[141] N. V. Tran,[141] L. Uplegger,[141] E. W. Vaandering,[141] C. Vernieri,[141] M. Verzocchi,[141] R. Vidal,[141] M. Wang,[141] H. A. Weber,[141] A. Whitbeck,[141] D. Acosta,[142] P. Avery,[142] P. Bortignon,[142] D. Bourilkov,[142] A. Brinkerhoff,[142] A. Carnes,[142] M. Carver,[142] D. Curry,[142] S. Das,[142] R. D. Field,[142] I. K. Furic,[142] J. Konigsberg,[142] A. Korytov,[142] P. Ma,[142] K. Matchev,[142] H. Mei,[142] P. Milenovic,[142,ppp] G. Mitselmakher,[142] D. Rank,[142] L. Shchutska,[142] D. Sperka,[142] L. Thomas,[142] J. Wang,[142] S. Wang,[142] J. Yelton,[142] S. Linn,[143] P. Markowitz,[143] G. Martinez,[143] J. L. Rodriguez,[143] A. Ackert,[144] J. R. Adams,[144] T. Adams,[144] A. Askew,[144] S. Bein,[144] B. Diamond,[144] S. Hagopian,[144] V. Hagopian,[144] K. F. Johnson,[144] A. Khatiwada,[144] H. Prosper,[144] A. Santra,[144] M. Weinberg,[144] M. M. Baarmand,[145] V. Bhopatkar,[145] S. Colafranceschi,[145,qqq] M. Hohlmann,[145] D. Noonan,[145] T. Roy,[145] F. Yumiceva,[145] M. R. Adams,[146] L. Apanasevich,[146] D. Berry,[146] R. R. Betts,[146] I. Bucinskaite,[146] R. Cavanaugh,[146] O. Evdokimov,[146] L. Gauthier,[146] C. E. Gerber,[146] D. J. Hofman,[146] P. Kurt,[146] C. O'Brien,[146] I. D. Sandoval Gonzalez,[146] P. Turner,[146] N. Varelas,[146] H. Wang,[146] Z. Wu,[146] M. Zakaria,[146] J. Zhang,[146] B. Bilki,[147,rrr] W. Clarida,[147] K. Dilsiz,[147] S. Durgut,[147] R. P. Gandrajula,[147] M. Haytmyradov,[147] V. Khristenko,[147] J.-P. Merlo,[147] H. Mermerkaya,[147,sss] A. Mestvirishvili,[147] A. Moeller,[147] J. Nachtman,[147] H. Ogul,[147] Y. Onel,[147] F. Ozok,[147,ttt] A. Penzo,[147] C. Snyder,[147] E. Tiras,[147] J. Wetzel,[147] K. Yi,[147] I. Anderson,[148] B. Blumenfeld,[148] A. Cocoros,[148] N. Eminizer,[148] D. Fehling,[148] L. Feng,[148] A. V. Gritsan,[148] P. Maksimovic,[148] M. Osherson,[148] J. Roskes,[148] U. Sarica,[148] M. Swartz,[148] M. Xiao,[148] Y. Xin,[148] C. You,[148] A. Al-bataineh,[149] P. Baringer,[149] A. Bean,[149] S. Boren,[149] J. Bowen,[149] C. Bruner,[149] J. Castle,[149] L. Forthomme,[149] R. P. Kenny III,[149] A. Kropivnitskaya,[149] D. Majumder,[149] W. Mcbrayer,[149] M. Murray,[149] S. Sanders,[149] R. Stringer,[149] J. D. Tapia Takaki,[149] Q. Wang,[149] A. Ivanov,[150] K. Kaadze,[150] S. Khalil,[150] M. Makouski,[150] Y. Maravin,[150] A. Mohammadi,[150] L. K. Saini,[150] N. Skhirtladze,[150] S. Toda,[150] F. Rebassoo,[151] D. Wright,[151] C. Anelli,[152] A. Baden,[152] O. Baron,[152] A. Belloni,[152] B. Calvert,[152] S. C. Eno,[152] C. Ferraioli,[152] J. A. Gomez,[152] N. J. Hadley,[152] S. Jabeen,[152] R. G. Kellogg,[152] T. Kolberg,[152] J. Kunkle,[152] Y. Lu,[152] A. C. Mignerey,[152] Y. H. Shin,[152] A. Skuja,[152] M. B. Tonjes,[152] S. C. Tonwar,[152] D. Abercrombie,[153] B. Allen,[153] A. Apyan,[153] R. Barbieri,[153] A. Baty,[153] R. Bi,[153] K. Bierwagen,[153] S. Brandt,[153] W. Busza,[153] I. A. Cali,[153] Z. Demiragli,[153] L. Di Matteo,[153] G. Gomez Ceballos,[153] M. Goncharov,[153] D. Hsu,[153] Y. Iiyama,[153] G. M. Innocenti,[153] M. Klute,[153] D. Kovalskyi,[153] K. Krajczar,[153] Y. S. Lai,[153] Y.-J. Lee,[153] A. Levin,[153] P. D. Luckey,[153] A. C. Marini,[153] C. Mcginn,[153] C. Mironov,[153] S. Narayanan,[153] X. Niu,[153] C. Paus,[153] C. Roland,[153] G. Roland,[153] J. Salfeld-Nebgen,[153] G. S. F. Stephans,[153] K. Sumorok,[153] K. Tatar,[153] M. Varma,[153] D. Velicanu,[153] J. Veverka,[153] J. Wang,[153] T. W. Wang,[153] B. Wyslouch,[153] M. Yang,[153] V. Zhukova,[153] A. C. Benvenuti,[154]

R. M. Chatterjee,[154] A. Evans,[154] A. Finkel,[154] A. Gude,[154] P. Hansen,[154] S. Kalafut,[154] S. C. Kao,[154] Y. Kubota,[154] Z. Lesko,[154] J. Mans,[154] S. Nourbakhsh,[154] N. Ruckstuhl,[154] R. Rusack,[154] N. Tambe,[154] J. Turkewitz,[154] J. G. Acosta,[155] S. Oliveros,[155] E. Avdeeva,[156] R. Bartek,[156] K. Bloom,[156] D. R. Claes,[156] A. Dominguez,[156] C. Fangmeier,[156] R. Gonzalez Suarez,[156] R. Kamalieddin,[156] I. Kravchenko,[156] A. Malta Rodrigues,[156] F. Meier,[156] J. Monroy,[156] J. E. Siado,[156] G. R. Snow,[156] B. Stieger,[156] M. Alyari,[157] J. Dolen,[157] J. George,[157] A. Godshalk,[157] C. Harrington,[157] I. Iashvili,[157] J. Kaisen,[157] A. Kharchilava,[157] A. Kumar,[157] A. Parker,[157] S. Rappoccio,[157] B. Roozbahani,[157] G. Alverson,[158] E. Barberis,[158] D. Baumgartel,[158] A. Hortiangtham,[158] B. Knapp,[158] A. Massironi,[158] D. M. Morse,[158] D. Nash,[158] T. Orimoto,[158] R. Teixeira De Lima,[158] D. Trocino,[158] R.-J. Wang,[158] D. Wood,[158] S. Bhattacharya,[159] K. A. Hahn,[159] A. Kubik,[159] A. Kumar,[159] J. F. Low,[159] N. Mucia,[159] N. Odell,[159] B. Pollack,[159] M. H. Schmitt,[159] K. Sung,[159] M. Trovato,[159] M. Velasco,[159] N. Dev,[160] M. Hildreth,[160] K. Hurtado Anampa,[160] C. Jessop,[160] D. J. Karmgard,[160] N. Kellams,[160] K. Lannon,[160] N. Marinelli,[160] F. Meng,[160] C. Mueller,[160] Y. Musienko,[160,ll] M. Planer,[160] A. Reinsvold,[160] R. Ruchti,[160] G. Smith,[160] S. Taroni,[160] M. Wayne,[160] M. Wolf,[160] A. Woodard,[160] J. Alimena,[161] L. Antonelli,[161] J. Brinson,[161] B. Bylsma,[161] L. S. Durkin,[161] S. Flowers,[161] B. Francis,[161] A. Hart,[161] C. Hill,[161] R. Hughes,[161] W. Ji,[161] B. Liu,[161] W. Luo,[161] D. Puigh,[161] B. L. Winer,[161] H. W. Wulsin,[161] S. Cooperstein,[162] O. Driga,[162] P. Elmer,[162] J. Hardenbrook,[162] P. Hebda,[162] D. Lange,[162] J. Luo,[162] D. Marlow,[162] T. Medvedeva,[162] K. Mei,[162] M. Mooney,[162] J. Olsen,[162] C. Palmer,[162] P. Piroué,[162] D. Stickland,[162] C. Tully,[162] A. Zuranski,[162] S. Malik,[163] A. Barker,[164] V. E. Barnes,[164] S. Folgueras,[164] L. Gutay,[164] M. K. Jha,[164] M. Jones,[164] A. W. Jung,[164] K. Jung,[164] D. H. Miller,[164] N. Neumeister,[164] X. Shi,[164] J. Sun,[164] A. Svyatkovskiy,[164] F. Wang,[164] W. Xie,[164] L. Xu,[164] N. Parashar,[165] J. Stupak,[165] A. Adair,[166] B. Akgun,[166] Z. Chen,[166] K. M. Ecklund,[166] F. J. M. Geurts,[166] M. Guilbaud,[166] W. Li,[166] B. Michlin,[166] M. Northup,[166] B. P. Padley,[166] R. Redjimi,[166] J. Roberts,[166] J. Rorie,[166] Z. Tu,[166] J. Zabel,[166] B. Betchart,[167] A. Bodek,[167] P. de Barbaro,[167] R. Demina,[167] Y. t. Duh,[167] T. Ferbel,[167] M. Galanti,[167] A. Garcia-Bellido,[167] J. Han,[167] O. Hindrichs,[167] A. Khukhunaishvili,[167] K. H. Lo,[167] P. Tan,[167] M. Verzetti,[167] J. P. Chou,[168] E. Contreras-Campana,[168] Y. Gershtein,[168] T. A. Gómez Espinosa,[168] E. Halkiadakis,[168] M. Heindl,[168] D. Hidas,[168] E. Hughes,[168] S. Kaplan,[168] R. Kunnawalkam Elayavalli,[168] S. Kyriacou,[168] A. Lath,[168] K. Nash,[168] H. Saka,[168] S. Salur,[168] S. Schnetzer,[168] D. Sheffield,[168] S. Somalwar,[168] R. Stone,[168] S. Thomas,[168] P. Thomassen,[168] M. Walker,[168] M. Foerster,[169] J. Heideman,[169] G. Riley,[169] K. Rose,[169] S. Spanier,[169] K. Thapa,[169] O. Bouhali,[170,uuu] A. Celik,[170] M. Dalchenko,[170] M. De Mattia,[170] A. Delgado,[170] S. Dildick,[170] R. Eusebi,[170] J. Gilmore,[170] T. Huang,[170] E. Juska,[170] T. Kamon,[170,vvv] R. Mueller,[170] Y. Pakhotin,[170] R. Patel,[170] A. Perloff,[170] L. Perniè,[170] D. Rathjens,[170] A. Rose,[170] A. Safonov,[170] A. Tatarinov,[170] K. A. Ulmer,[170] N. Akchurin,[171] C. Cowden,[171] J. Damgov,[171] C. Dragoiu,[171] P. R. Dudero,[171] J. Faulkner,[171] S. Kunori,[171] K. Lamichhane,[171] S. W. Lee,[171] T. Libeiro,[171] S. Undleeb,[171] I. Volobouev,[171] Z. Wang,[171] A. G. Delannoy,[172] S. Greene,[172] A. Gurrola,[172] R. Janjam,[172] W. Johns,[172] C. Maguire,[172] A. Melo,[172] H. Ni,[172] P. Sheldon,[172] S. Tuo,[172] J. Velkovska,[172] Q. Xu,[172] M. W. Arenton,[173] P. Barria,[173] B. Cox,[173] J. Goodell,[173] R. Hirosky,[173] A. Ledovskoy,[173] H. Li,[173] C. Neu,[173] T. Sinthuprasith,[173] Y. Wang,[173] E. Wolfe,[173] F. Xia,[173] C. Clarke,[174] R. Harr,[174] P. E. Karchin,[174] P. Lamichhane,[174] J. Sturdy,[174] D. A. Belknap,[175] S. Dasu,[175] L. Dodd,[175] S. Duric,[175] B. Gomber,[175] M. Grothe,[175] M. Herndon,[175] A. Hervé,[175] P. Klabbers,[175] A. Lanaro,[175] A. Levine,[175] K. Long,[175] R. Loveless,[175] I. Ojalvo,[175] T. Perry,[175] G. A. Pierro,[175] G. Polese,[175] T. Ruggles,[175] A. Savin,[175] A. Sharma,[175] N. Smith,[175] W. H. Smith,[175] D. Taylor,[175] and N. Woods[175]

(CMS Collaboration)

[1]*Yerevan Physics Institute, Yerevan, Armenia*
[2]*Institut für Hochenergiephysik, Wien, Austria*
[3]*National Centre for Particle and High Energy Physics, Minsk, Belarus*
[4]*Universiteit Antwerpen, Antwerpen, Belgium*
[5]*Vrije Universiteit Brussel, Brussel, Belgium*
[6]*Université Libre de Bruxelles, Bruxelles, Belgium*
[7]*Ghent University, Ghent, Belgium*
[8]*Université Catholique de Louvain, Louvain-la-Neuve, Belgium*
[9]*Université de Mons, Mons, Belgium*
[10]*Centro Brasileiro de Pesquisas Fisicas, Rio de Janeiro, Brazil*
[11]*Universidade do Estado do Rio de Janeiro, Rio de Janeiro, Brazil*
[12a]*Universidade Estadual Paulista, São Paulo, Brazil*

[12b]*Universidade Federal do ABC, São Paulo, Brazil*
[13]*Institute for Nuclear Research and Nuclear Energy, Sofia, Bulgaria*
[14]*University of Sofia, Sofia, Bulgaria*
[15]*Beihang University, Beijing, China*
[16]*Institute of High Energy Physics, Beijing, China*
[17]*State Key Laboratory of Nuclear Physics and Technology, Peking University, Beijing, China*
[18]*Universidad de Los Andes, Bogota, Colombia*
[19]*University of Split, Faculty of Electrical Engineering, Mechanical Engineering and Naval Architecture, Split, Croatia*
[20]*University of Split, Faculty of Science, Split, Croatia*
[21]*Institute Rudjer Boskovic, Zagreb, Croatia*
[22]*University of Cyprus, Nicosia, Cyprus*
[23]*Charles University, Prague, Czech Republic*
[24]*Universidad San Francisco de Quito, Quito, Ecuador*
[25]*Academy of Scientific Research and Technology of the Arab Republic of Egypt, Egyptian Network of High Energy Physics, Cairo, Egypt*
[26]*National Institute of Chemical Physics and Biophysics, Tallinn, Estonia*
[27]*Department of Physics, University of Helsinki, Helsinki, Finland*
[28]*Helsinki Institute of Physics, Helsinki, Finland*
[29]*Lappeenranta University of Technology, Lappeenranta, Finland*
[30]*IRFU, CEA, Université Paris-Saclay, Gif-sur-Yvette, France*
[31]*Laboratoire Leprince-Ringuet, Ecole Polytechnique, IN2P3-CNRS, Palaiseau, France*
[32]*Institut Pluridisciplinaire Hubert Curien, Université de Strasbourg, Université de Haute Alsace Mulhouse, CNRS/IN2P3, Strasbourg, France*
[33]*Centre de Calcul de l'Institut National de Physique Nucleaire et de Physique des Particules, CNRS/IN2P3, Villeurbanne, France*
[34]*Université de Lyon, Université Claude Bernard Lyon 1, CNRS-IN2P3, Institut de Physique Nucléaire de Lyon, Villeurbanne, France*
[35]*Georgian Technical University, Tbilisi, Georgia*
[36]*Tbilisi State University, Tbilisi, Georgia*
[37]*RWTH Aachen University, I. Physikalisches Institut, Aachen, Germany*
[38]*RWTH Aachen University, III. Physikalisches Institut A, Aachen, Germany*
[39]*RWTH Aachen University, III. Physikalisches Institut B, Aachen, Germany*
[40]*Deutsches Elektronen-Synchrotron, Hamburg, Germany*
[41]*University of Hamburg, Hamburg, Germany*
[42]*Institut für Experimentelle Kernphysik, Karlsruhe, Germany*
[43]*Institute of Nuclear and Particle Physics (INPP), NCSR Demokritos, Aghia Paraskevi, Greece*
[44]*National and Kapodistrian University of Athens, Athens, Greece*
[45]*University of Ioánnina, Ioánnina, Greece*
[46]*MTA-ELTE Lendület CMS Particle and Nuclear Physics Group, Eötvös Loránd University, Budapest, Hungary*
[47]*Wigner Research Centre for Physics, Budapest, Hungary*
[48]*Institute of Nuclear Research ATOMKI, Debrecen, Hungary*
[49]*University of Debrecen, Debrecen, Hungary*
[50]*National Institute of Science Education and Research, Bhubaneswar, India*
[51]*Panjab University, Chandigarh, India*
[52]*University of Delhi, Delhi, India*
[53]*Saha Institute of Nuclear Physics, Kolkata, India*
[54]*Indian Institute of Technology Madras, Madras, India*
[55]*Bhabha Atomic Research Centre, Mumbai, India*
[56]*Tata Institute of Fundamental Research-A, Mumbai, India*
[57]*Tata Institute of Fundamental Research-B, Mumbai, India*
[58]*Indian Institute of Science Education and Research (IISER), Pune, India*
[59]*Institute for Research in Fundamental Sciences (IPM), Tehran, Iran*
[60]*University College Dublin, Dublin, Ireland*
[61a]*INFN Sezione di Bari, Bari, Italy*
[61b]*Università di Bari, Bari, Italy*
[61c]*Politecnico di Bari, Bari, Italy*
[62a]*INFN Sezione di Bologna, Bologna, Italy*
[62b]*Università di Bologna, Bologna, Italy*

[63a]*INFN Sezione di Catania, Catania, Italy*
[63b]*Università di Catania, Catania, Italy*
[64a]*INFN Sezione di Firenze, Firenze, Italy*
[64b]*Università di Firenze, Firenze, Italy*
[65]*INFN Laboratori Nazionali di Frascati, Frascati, Italy*
[66a]*INFN Sezione di Genova, Genova, Italy*
[66b]*Università di Genova, Genova, Italy*
[67a]*INFN Sezione di Milano-Bicocca, Milano, Italy*
[67b]*Università di Milano-Bicocca, Milano, Italy*
[68a]*INFN Sezione di Napoli, Roma, Italy*
[68b]*Università di Napoli 'Federico II', Roma, Italy*
[68c]*Università della Basilicata, Roma, Italy*
[68d]*Università G. Marconi, Roma, Italy*
[69a]*INFN Sezione di Padova, Padova, Italy*
[69b]*Università di PadovaPadova, Italy*
[69c]*Università di Trento, Trento, Italy*
[70a]*INFN Sezione di Pavia, Pavia, Italy*
[70b]*Università di Pavia, Pavia, Italy*
[71a]*INFN Sezione di Perugia, Perugia, Italy*
[71b]*Università di Perugia, Perugia, Italy*
[72a]*INFN Sezione di Pisa, Pisa, Italy*
[72b]*Università di Pisa, Pisa, Italy*
[72c]*Scuola Normale Superiore di Pisa, Pisa, Italy*
[73a]*INFN Sezione di Roma, Roma, Italy*
[73b]*Università di Roma, Roma, Italy*
[74a]*INFN Sezione di Torino, Torino, Italy*
[74b]*Università di Torino, Torino, Italy*
[74c]*Università del Piemonte Orientale, Novara, Italy*
[75a]*INFN Sezione di Trieste, Trieste, Italy*
[75b]*Università di Trieste, Trieste, Italy*
[76]*Kyungpook National University, Daegu, Korea*
[77]*Chonbuk National University, Jeonju, Korea*
[78]*Hanyang University, Seoul, Korea*
[79]*Korea University, Seoul, Korea*
[80]*Seoul National University, Seoul, Korea*
[81]*University of Seoul, Seoul, Korea*
[82]*Sungkyunkwan University, Suwon, Korea*
[83]*Vilnius University, Vilnius, Lithuania*
[84]*National Centre for Particle Physics, Universiti Malaya, Kuala Lumpur, Malaysia*
[85]*Centro de Investigacion y de Estudios Avanzados del IPN, Mexico City, Mexico*
[86]*Universidad Iberoamericana, Mexico City, Mexico*
[87]*Benemerita Universidad Autonoma de Puebla, Puebla, Mexico*
[88]*Universidad Autónoma de San Luis Potosí, San Luis Potosí, Mexico*
[89]*University of Auckland, Auckland, New Zealand*
[90]*University of Canterbury, Christchurch, New Zealand*
[91]*National Centre for Physics, Quaid-I-Azam University, Islamabad, Pakistan*
[92]*National Centre for Nuclear Research, Swierk, Poland*
[93]*Institute of Experimental Physics, Faculty of Physics, University of Warsaw, Warsaw, Poland*
[94]*Laboratório de Instrumentação e Física Experimental de Partículas, Lisboa, Portugal*
[95]*Joint Institute for Nuclear Research, Dubna, Russia*
[96]*Petersburg Nuclear Physics Institute, Gatchina (St. Petersburg), Russia*
[97]*Institute for Nuclear Research, Moscow, Russia*
[98]*Institute for Theoretical and Experimental Physics, Moscow, Russia*
[99]*Moscow Institute of Physics and Technology, Moscow, Russia*
[100]*National Research Nuclear University 'Moscow Engineering Physics Institute' (MEPhI), Moscow, Russia*
[101]*P. N. Lebedev Physical Institute, Moscow, Russia*
[102]*Skobeltsyn Institute of Nuclear Physics, Lomonosov Moscow State University, Moscow, Russia*
[103]*Novosibirsk State University (NSU), Novosibirsk, Russia*
[104]*State Research Center of Russian Federation, Institute for High Energy Physics, Protvino, Russia*

[105]*University of Belgrade, Faculty of Physics and Vinca Institute of Nuclear Sciences, Belgrade, Serbia*
[106]*Centro de Investigaciones Energéticas Medioambientales y Tecnológicas (CIEMAT), Madrid, Spain*
[107]*Universidad Autónoma de Madrid, Madrid, Spain*
[108]*Universidad de Oviedo, Oviedo, Spain*
[109]*Instituto de Física de Cantabria (IFCA), CSIC-Universidad de Cantabria, Santander, Spain*
[110]*CERN, European Organization for Nuclear Research, Geneva, Switzerland*
[111]*Paul Scherrer Institut, Villigen, Switzerland*
[112]*Institute for Particle Physics, ETH Zurich, Zurich, Switzerland*
[113]*Universität Zürich, Zurich, Switzerland*
[114]*National Central University, Chung-Li, Taiwan*
[115]*National Taiwan University (NTU), Taipei, Taiwan*
[116]*Chulalongkorn University, Faculty of Science, Department of Physics, Bangkok, Thailand*
[117]*Cukurova University, Adana, Turkey*
[118]*Middle East Technical University, Physics Department, Ankara, Turkey*
[119]*Bogazici University, Istanbul, Turkey*
[120]*Istanbul Technical University, Istanbul, Turkey*
[121]*Institute for Scintillation Materials of National Academy of Science of Ukraine, Kharkov, Ukraine*
[122]*National Scientific Center, Kharkov Institute of Physics and Technology, Kharkov, Ukraine*
[123]*University of Bristol, Bristol, United Kingdom*
[124]*Rutherford Appleton Laboratory, Didcot, United Kingdom*
[125]*Imperial College, London, United Kingdom*
[126]*Brunel University, Uxbridge, United Kingdom*
[127]*Baylor University, Waco, Texas, USA*
[128]*The University of Alabama, Tuscaloosa, Alabama, USA*
[129]*Boston University, Boston, USA*
[130]*Brown University, Providence, USA*
[131]*University of California, Davis, Davis, California, USA*
[132]*University of California, Los Angeles, California, USA*
[133]*University of California, Riverside, Riverside, California, USA*
[134]*University of California, San Diego, La Jolla, USA*
[135]*University of California, Santa Barbara—Department of Physics, Santa Barbara, California, USA*
[136]*California Institute of Technology, Pasadena, California, USA*
[137]*Carnegie Mellon University, Pittsburgh, Pennsylvania, USA*
[138]*University of Colorado Boulder, Boulder, Colorado, USA*
[139]*Cornell University, Ithaca, New York, USA*
[140]*Fairfield University, Fairfield, Connecticut, USA*
[141]*Fermi National Accelerator Laboratory, Batavia, New York, USA*
[142]*University of Florida, Gainesville, Florida, USA*
[143]*Florida International University, Miami, Florida, USA*
[144]*Florida State University, Tallahassee, Florida, USA*
[145]*Florida Institute of Technology, Melbourne, Florida, USA*
[146]*University of Illinois at Chicago (UIC), Chicago, Illinois, USA*
[147]*The University of Iowa, Iowa City, Iowa, USA*
[148]*Johns Hopkins University, Baltimore, Maryland, USA*
[149]*The University of Kansas, Lawrence, Kansas, USA*
[150]*Kansas State University, Manhattan, Kansas, USA*
[151]*Lawrence Livermore National Laboratory, Livermore, California, USA*
[152]*University of Maryland, College Park, Maryland, USA*
[153]*Massachusetts Institute of Technology, Cambridge, Massachusetts, USA*
[154]*University of Minnesota, Minneapolis, Minnesota, USA*
[155]*University of Mississippi, Oxford, Mississippi, USA*
[156]*University of Nebraska-Lincoln, Lincoln, Nebraska, USA*
[157]*State University of New York at Buffalo, Buffalo, New York, USA*
[158]*Northeastern University, Boston, Massachusetts, USA*
[159]*Northwestern University, Evanston, Illinois, USA*
[160]*University of Notre Dame, Notre Dame, Indiana, USA*
[161]*The Ohio State University, Columbus, Ohio, USA*
[162]*Princeton University, Princeton, New Jersey, USA*
[163]*University of Puerto Rico, Mayaguez, Puerto Rico, USA*
[164]*Purdue University, West Lafayette, Indiana, USA*

[165]*Purdue University Calumet, Hammond, Indiana, USA*
[166]*Rice University, Houston, Texas, USA*
[167]*University of Rochester, Rochester, New York, USA*
[168]*Rutgers, The State University of New Jersey, Piscataway, New Jersey, USA*
[169]*University of Tennessee, Knoxville, Tennessee, USA*
[170]*Texas A&M University, College Station, Texas, USA*
[171]*Texas Tech University, Lubbock, Texas, USA*
[172]*Vanderbilt University, Nashville, Tennessee, USA*
[173]*University of Virginia, Charlottesville, Virginia, USA*
[174]*Wayne State University, Detroit, Michigan, USA*
[175]*University of Wisconsin—Madison, Madison, Wisconsin, USA*

[a]Deceased.
[b]Also at Vienna University of Technology, Vienna, Austria.
[c]Also at State Key Laboratory of Nuclear Physics and Technology, Peking University, Beijing, China.
[d]Also at Institut Pluridisciplinaire Hubert Curien, Université de Strasbourg, Université de Haute Alsace Mulhouse, CNRS/IN2P3, Strasbourg, France.
[e]Also at Universidade Estadual de Campinas, Campinas, Brazil.
[f]Also at Universidade Federal de Pelotas, Pelotas, Brazil.
[g]Also at Université Libre de Bruxelles, Bruxelles, Belgium.
[h]Also at Deutsches Elektronen-Synchrotron, Hamburg, Germany.
[i]Also at Joint Institute for Nuclear Research, Dubna, Russia.
[j]Also at Suez University, Suez, Egypt.
[k]Also at British University in Egypt, Cairo, Egypt.
[l]Also at Ain Shams University, Cairo, Egypt.
[m]Also at Helwan University, Cairo, Egypt.
[n]Also at Université de Haute Alsace, Mulhouse, France.
[o]Also at CERN, European Organization for Nuclear Research, Geneva, Switzerland.
[p]Also at Skobeltsyn Institute of Nuclear Physics, Lomonosov Moscow State University, Moscow, Russia.
[q]Also at Tbilisi State University, Tbilisi, Georgia.
[r]Also at RWTH Aachen University, III. Physikalisches Institut A, Aachen, Germany.
[s]Also at University of Hamburg, Hamburg, Germany.
[t]Also at Brandenburg University of Technology, Cottbus, Germany.
[u]Also at Institute of Nuclear Research ATOMKI, Debrecen, Hungary.
[v]Also at MTA-ELTE Lendület CMS Particle and Nuclear Physics Group, Eötvös Loránd University, Budapest, Hungary.
[w]Also at University of Debrecen, Debrecen, Hungary.
[x]Also at Indian Institute of Science Education and Research, Bhopal, India.
[y]Also at Institute of Physics, Bhubaneswar, India.
[z]Also at University of Visva-Bharati, Santiniketan, India.
[aa]Also at University of Ruhuna, Matara, Sri Lanka.
[bb]Also at Isfahan University of Technology, Isfahan, Iran.
[cc]Also at University of Tehran, Department of Engineering Science, Tehran, Iran.
[dd]Also at Yazd University, Yazd, Iran.
[ee]Also at Plasma Physics Research Center, Science and Research Branch, Islamic Azad University, Tehran, Iran.
[ff]Also at Università degli Studi di Siena, Siena, Italy.
[gg]Also at Purdue University, West Lafayette, USA.
[hh]Also at International Islamic University of Malaysia, Kuala Lumpur, Malaysia.
[ii]Also at Malaysian Nuclear Agency, MOSTI, Kajang, Malaysia.
[jj]Also at Consejo Nacional de Ciencia y Tecnología, Mexico city, Mexico.
[kk]Also at Warsaw University of Technology, Institute of Electronic Systems, Warsaw, Poland.
[ll]Also at Institute for Nuclear Research, Moscow, Russia.
[mm]Also at National Research Nuclear University 'Moscow Engineering Physics Institute' (MEPhI), Moscow, Russia.
[nn]Also at St. Petersburg State Polytechnical University, St. Petersburg, Russia.
[oo]Also at University of Florida, Gainesville, USA.
[pp]Also at P. N. Lebedev Physical Institute, Moscow, Russia.
[qq]Also at California Institute of Technology, Pasadena, USA.
[rr]Also at Budker Institute of Nuclear Physics, Novosibirsk, Russia.
[ss]Also at Faculty of Physics, University of Belgrade, Belgrade, Serbia.
[tt]Also at INFN Sezione di Roma, Università di Roma, Roma, Italy.
[uu]Also at Scuola Normale e Sezione dell'INFN, Pisa, Italy.

[vv]Also at National and Kapodistrian University of Athens, Athens, Greece.
[ww]Also at Riga Technical University, Riga, Latvia.
[xx]Also at Institute for Theoretical and Experimental Physics, Moscow, Russia.
[yy]Also at Albert Einstein Center for Fundamental Physics, Bern, Switzerland.
[zz]Also at Gaziosmanpasa University, Tokat, Turkey.
[aaa]Also at Adiyaman University, Adiyaman, Turkey.
[bbb]Also at Mersin University, Mersin, Turkey.
[ccc]Also at Cag University, Mersin, Turkey.
[ddd]Also at Piri Reis University, Istanbul, Turkey.
[eee]Also at Ozyegin University, Istanbul, Turkey.
[fff]Also at Izmir Institute of Technology, Izmir, Turkey.
[ggg]Also at Marmara University, Istanbul, Turkey.
[hhh]Also at Kafkas University, Kars, Turkey.
[iii]Also at Istanbul Bilgi University, Istanbul, Turkey.
[jjj]Also at Yildiz Technical University, Istanbul, Turkey.
[kkk]Also at Hacettepe University, Ankara, Turkey.
[lll]Also at Rutherford Appleton Laboratory, Didcot, United Kingdom.
[mmm]Also at School of Physics and Astronomy, University of Southampton, Southampton, United Kingdom.
[nnn]Also at Instituto de Astrofísica de Canarias, La Laguna, Spain.
[ooo]Also at Utah Valley University, Orem, USA.
[ppp]Also at University of Belgrade, Faculty of Physics and Vinca Institute of Nuclear Sciences, Belgrade, Serbia.
[qqq]Also at Facoltà Ingegneria, Università di Roma, Roma, Italy.
[rrr]Also at Argonne National Laboratory, Argonne, USA.
[sss]Also at Erzincan University, Erzincan, Turkey.
[ttt]Also at Mimar Sinan University, Istanbul, Istanbul, Turkey.
[uuu]Also at Texas A&M University at Qatar, Doha, Qatar.
[vvv]Also at Kyungpook National University, Daegu, Korea.